Journal Pre-proof

Structural characterization of almond polysaccharides (Armeniaca Sibirica L. Lam) and the prebiotic effects on human intestinal flora

Yanqi Peng, Ji Wu, Mingyue Ma, Yuzhen Pi, Xiqing Yue, Yanyu Peng

PII: S0308-8146(25)04083-X

DOI: https://doi.org/10.1016/j.foodchem.2025.146831

Reference: FOCH 146831

To appear in: *Food Chemistry*

Received date: 2 July 2025

Revised date: 12 October 2025

Accepted date: 23 October 2025

Please cite this article as: Y. Peng, J. Wu, M. Ma, et al., Structural characterization of almond polysaccharides (Armeniaca Sibirica L. Lam) and the prebiotic effects on human intestinal flora, *Food Chemistry* (2024), https://doi.org/10.1016/j.foodchem.2025.146831

Structural characterization of almond polysaccharides (*Armeniaca Sibirica* L. Lam) and the prebiotic effects on human intestinal flora

Authors: Yanqi Peng [a, b, e], Ji Wu [c, e], Mingyue Ma [a], Yuzhen Pi [b, *], Xiqing Yue [b, *], Yanyu Peng [d, e, *]

Affiliations:

[a] School of Public Health, Shenyang Medical College, Shenyang 110034, Liaoning Province, People's Republic of China.

[b] College of Food Science, Shenyang Agricultural University, Shenyang 110034, Liaoning Province, People's Republic of China.

[c] Shenyang Medical College, No.146 Yellow River North Street, Shenyang 110034, Liaoning Province, People's Republic of China.

[d] Department of Histology and Embryology, School of Basic Medicine, Shenyang Medical College, No.146 Yellow River North Street, Shenyang 110034, Liaoning Province, People's Republic of China.

[e] Shenyang Key Laboratory of Chronic Disease Assessment and Nutritional Intervention for Heart and Brain, Shenyang Medical College, Shenyang 110034, People's Republic of China.

***Corresponding Authors:**

Yuzhen Pi, Ph.D./ Associate Professor, College of Food Science, Shenyang Agricultural University, Shenyang 11086, China. E-mail: yuzhen_pi@sina.com

Xiqing Yue, Ph.D./ Professor, College of Food Science, Shenyang Agricultural University, Shenyang 11086, China. E-mail: yxqsyau@126.com

Yanyu Peng, Ph.D./ Lecturer, Department of Histology and Embryology, School of Basic Medicine, Shenyang Medical College, Shenyang 110034, China. E-mail: yypeng@cmu.edu.cn (ORCID:0000-0002-1858-2112)

Abstract

In this study, the prebiotic effect of polysaccharide AS-3 extracted from almond (*Armeniaca Sibirica* L. Lam) on the intestinal flora of healthy individuals was investigated. Structural characterization determined AS-3 has a molecular weight of approximately 51 kDa. Its composition includes arabinose, galactose, rhamnose, glucose, and glucuronic acid, adopting a triple helical structure. Detailed linkage analysis via NMR and methylation studies identified a primary backbone featuring →3,6)-α-D-Gal-(1→, →3)-β-D-Gal-(1→, and →5)-α-L-Araf-(1→ units. Branching occurs at the O-6 position of →3,6)-α-D-Gal-(1→ residues. Compared to inulin, AS-3 consistently yielded greater microbial diversity during both 24-hour and 48-hour fermentation experiments. GC-MS

analysis confirmed that AS-3 significantly boosts beneficial short-chain fatty acids (SCFAs), particularly acetic acid and butyric acid. It also selectively stimulated beneficial bacteria while suppressing potentially harmful ones. Significantly, AS-3 lowered the *Firmicutes/Bacteroidetes* ratio, suggesting a role in promoting gut balance. These findings support AS-3's potential for functional food applications targeting gut microecological health.

Keywords: Almond; Polysaccharides; Structural characterization; Gut microbiota; Probiotic effect

1. Introduction

In recent years, with the in-depth study of intestinal microecology, nutritional intervention strategies centered on ‘colony-host interactions’ have become a hotspot for improving metabolic diseases and immune functions. Natural polysaccharides, as a class of biomolecules with complex structures, have gradually become the focus of research in the field of functional foods and pharmaceuticals due to their unique prebiotic properties and regulatory functions on intestinal flora(Z. Zhu et al., 2024)(Hui et al., 2024). The structure of natural polysaccharides is diverse, and their monosaccharide composition, glycosidic bond type, and molecular weight distribution determine their unique biological functions(L. Zhu et al., 2025). Different extraction methods or purification means can significantly affect the structure and activity of polysaccharides, and

even if the same extraction method is used, batch differences in raw materials may lead to differences in the structure and activity of the resulting polysaccharides, which is an issue to be considered during the study (Zhai et al., 2025). Interestingly, even when the two polysaccharides were purified from the same plant rhizomes, they still differed dramatically, with acidic polysaccharides providing greater stimulation of macrophage activity and better modulation of the intestinal immune response than neutral polysaccharides.

In terms of modulation of the gut microbiota, polysaccharides have been shown to have a significant impact on the composition and diversity of the gut microbiota. For example, polysaccharides from *Cistanche* can promote the growth of beneficial bacteria and increase the production of short-chain fatty acids (SCFAs), which are essential for gut health and systemic metabolism (Lian et al., 2025). Similarly, polysaccharides from ganoderma lucidum spores inhibited obesity, hyperlipidaemia, inflammation and fat accumulation in mice, improved gut microbiota flora disruption, and maintained intestinal barrier function(Sang et al., 2021). In addition, polysaccharides that have been subjected to different heat treatments have very different effects on human intestinal flora(Liu et al., 2025). It has been shown that there is also a constitutive relationship between polysaccharides and flora regulation. The galactose-rich Ganoderma lucidum polysaccharides may enhance immune function and improve the composition of the intestinal microbiota by boosting beneficial bacteria such as *Lactobacillus* (Z.-W. Wu et al., 2025). Likewise, Deglet Noor polysaccharides, which are rich in mannose and glucose, significantly reduce blood sugar levels and reverse gut microbial disruption, increasing gut microbial

diversity(Ullah et al., 2025). Moreover, glucose-dominated polysaccharides may be preferentially utilized by the *Firmicutes*, affecting the distribution of the ratio of acetic acid to butyric acid(Fabiano et al., 2025).

Almond (*Armeniaca Sibirica* L. Lam), as a traditional food and medicinal ingredient, is not only a medicinal herb with the functions of relieving cough and asthma, laxative and laxative but also rich in polysaccharides, flavonoids, unsaturated fatty acids and other functional components as revealed by modern research (Özcan, 2023). Currently, research on almonds continues to focus on patients with metabolic syndrome. A randomized controlled trial reported that regular snacking on almonds improved intake of essential nutrients, lowered total cholesterol and low-density lipoprotein (LDL) cholesterol levels, and enhanced intestinal barrier function by reducing markers of intestinal inflammation(Beaver et al., 2025). These findings suggest that almonds may have good potential as a functional food in the management of chronic diseases such as metabolic syndrome(Beaver et al., 2025). In addition, almonds have the potential to revolutionize the culinary experience and nutritional value of food. For example, the unique almond-like aroma imparted to acidic whey through fermentation not only provides ideas for developing functional beverages with novel flavors but also expands the path of high-value utilization of dairy processing waste from an environmental perspective(Ragno et al., 2025). Meanwhile, research on the modification of almond gum polysaccharides continues to advance, exploring new ways to improve the texture and quality of food products by exploring their physicochemical properties(Paranthaman, 2025).

In the field of almond polysaccharides, we have already carried out relevant research work in the past. In the past, we extracted and purified almond polysaccharide AP-1 from the cold-pressed almond meal by hot water and column chromatography, and its monosaccharide composition was mainly glucose with small amounts of arabinose, galactose and mannose(Peng et al., 2023). It has been found that AP-1 enriches *Lactobacillus* and has a favorable ameliorative effect on DSS-induced ulcerative colitis in mice(Peng, Li, et al., 2024; Peng, Zhu, et al., 2024). Since only a single component of the almond crude polysaccharide extracted by the hot water method was obtained after purification, this may limit the in-depth exploration of the structural diversity and functional potential of almond polysaccharides. Thus, we hypothesized that AS-3, a triple-helix polysaccharide extracted from almonds, contained only trace amounts of glucose and had more vigorous prebiotic activity compared to inulin. Specifically, AS-3 has the potential to enhance the diversity of beneficial gut microbiota, increase the production of SCFAs, and regulate the ratio of *Firmicutes/Bacteroidetes* to maintain gut homeostasis in healthy individuals.

Therefore, the experiment is proposed to be further explored by the enzymatic digestion method, aiming to obtain novel almond polysaccharide components and comprehensively assess the functional value of almond polysaccharides through systematic structural analysis, combined with the evaluation of their prebiotic properties on human intestinal flora. To provide a more comprehensive scientific basis for its application in functional foods, intestinal health intervention and other fields.

2. Materials and methods

2.1. Materials and reagents

The by-products (almond pomace) after the extraction of almond oil by using cold pressing technology were provided by Xinglinchunxiao Chengde Biotechnology Co.

High-temperature α-amylase (4000 U/g), AB-8 macroporous adsorbent resin, DEAE-52 cellulose, and Sephadex G-100 dextran gel were purchased from Beijing Solarbio Biotechnology Co. (Beijing, China). Amyloglucosidase (260 U/mL) was purchased from Macklin Biochemical Technology Co. (Shanghai, China). Papain (100000 U/g), monosaccharide standard substances (fucose, rhamnose, arabinose, galactose, glucose, xylose, mannose, fructose, ribose, galacturonic acid, glucuronic acid, mannuronic acid and glucuronic acid) were purchased from Sigma Co. (Missouri, USA). The analytical standards of acetic acid, propionic acid, i-Butyric acid, n-Butyric acid, i-Valeric acid, n-Valeric acid, and caproic acid were all purchased from Shanghai Aladdin Biotechnology Co., Ltd. (Shanghai, China). Hexane (AR, 97%, Mw 86.18), trichloromethane (AR, 99.9%, Mw 119.38), n-butanol (GR, 99.8%, Mw 74.12), anhydrous ethanol (AR, 99.7%, Mw 46.07), phenol (AR, 99%, Mw 94.11), and sulfuric acid (GR, 98%, Mw 98.07) were all purchased from Sinopharm Group (Shanghai, China).

2.2. Extraction and isolation of ASDF and AS-3

The almond pomace was ground in a grinder and sieved through a 100-mesh sieve (0.15 mm) to obtain the almond powder, which was sealed and divided into sample bags and stored in a -80 ℃ refrigerator. Before use, the almond meal was dried at 50 °C for 24 hours and sieved again. The extraction steps of almond polysaccharides were shown in Fig. 1A. Specifically, 100 g of almond powder was first added to hexane (1:3, v/v) and stirred rapidly for about 3 hours. The procedure was repeated three to four times. After filtration, it was dried at 50 ℃ for 24 hours to obtain defatted almond powder.

After weighing 60 g of defatted almond powder, adding deionized water, adjusting the material-liquid ratio to 1:30, regulating the pH value to 6, adding high-temperature α-amylase 100 U/g (w/w), and heating in a water bath at 95 ℃ for 1 h, regulating the pH value to 6 again, adding papain (1%, w/v), and inactivating the enzyme in a 50 ℃ water bath for 1 h. The enzyme was inactivated by boiling water bath and centrifuged. The pH of the supernatant was adjusted to 4.2, adding amyloglucosidase 200 U/g (w/w), and a water bath at 60 ℃ for 1 h. The enzyme was inactivated by boiling water bath again and centrifuged. Secondary deproteinization was carried out using the Sevag reagent (trichloromethane: n-butanol = 4:1, v/v), which was repeated three times until no white precipitate appeared and concentrated under reduced pressure to remove the residual organic reagent. It was

decolorized with macroporous resin AB-8 (macroporous resin: polysaccharide solution=1:4, v/v), shaken at 37 ℃ for 1 h. The filtrate was collected by filtration, and the precipitate was collected by adding 95 % ethanol solution (1:4, v/v) and refrigerated overnight. The precipitate was dissolved and put into a 3500 Da dialysis bag, and then freeze-dried after dialysis treatment for 72 h. The almond crude polysaccharide ASDF was obtained.

Weighed 150 mg of almond crude polysaccharide ASDF dissolved in 17 mL of purified water, centrifuged at 10,000 r/min for 10 min, passed through 0.45 μm aqueous filtration membrane and then uploaded to the sample. Elution was performed sequentially with purified water, 0.1 M, 0.2 M and 0.3 M NaCl (1 mL/min, 5 mL/tube). The total sugar content of the collected solution was detected, and the absorbance curve was plotted. The collected fractions were evaporated at 40 ℃ under reduced pressure, dialyzed for 72 h and freeze-dried, weighed 70 mg of the above-lyophilized sample, dissolved in 5 mL of 0.1 M NaCl, centrifuged and filtered through the membrane and loaded. The flow rate was 0.4 mL/min, and one tube was collected every 10 min. The final selected tubes were combined, concentrated, dialyzed and lyophilized. The total sugar content was determined by the phenol sulfuric acid method(Yue et al., 2022), and the uronic acid content was determined by the m-hydroxyphenyl method(Ji et al., 2023).

2.3 Structural characterization of the almond polysaccharide AS-3

2.3.1 UV spectral

The UV-visible spectrum of AS-3 aqueous solution (1 mg/mL) was measured using a UV-visible spectrophotometer in the wavelength range of 220 - 400 nm.

2.3.2 Molecular weight and molecular configuration determination

The molecular weight and molecular configuration of AS-3 were determined using the SEC-MALLS-RI system concerning previous methods(L. Wang, Zhang, et al., 2018). Briefly, measurements of the weight-averaged molecular weight (Mw), number-averaged molecular weight (Mn), and polydispersity index (Mw/Mn) were carried out using a DAWN HELEOS-II laser photometer in an aqueous solution of $NaNO_3$ (0.1 M) containing 0.02 % NaN_3.

2.3.3 Determination of monosaccharide composition

The monosaccharide composition was determined by reference to the previous method with minor modifications(H. Zhang et al., 2021). Briefly, AS-3 was analyzed by high-performance anion exchange chromatography (HPAEC) on a CarboPac PA-20 anion-exchange column using a pulsed amperometric detector with a flow rate of 0.5 mL/min and an injection volume of 5 μL.

2.3.4 Determination of FTIR spectra

FT-IR was measured using a spectrometer following previous studies(S. Zhou et al., 2021). AS-3 was mixed with KBr powder and pressed into 1 mm pellets in the range of 400 - 400 cm^{-1}.

2.3.5 Scanning electron microscopy (SEM)

AS-3 was taken in small quantities on conductive carbon tape, sprayed with gold and then scanned and photographed using an electron microscope with a magnification of 100 - 4000 times.

2.3.6 Determination of triple-stranded helical structure

Referring to the previous method(Villares, 2013), an equal volume of polysaccharide solution was thoroughly mixed with Congo red reagent, the NaOH concentration in the mixture was adjusted to the range of 0 - 0.5 M with NaOH solution, scanned in 400 - 700 nm and the maximum absorption wavelength was recorded.

2.3.7 Methylation and GC-MS

Using the previous method with slight modification(Peng et al., 2023), specifically, AS-3 was dissolved in DMSO, hydrolyzed using

TFA (2 mol/L) at 121 ℃ for 1.5 h, then reduced using $NaBD_4$, and finally acetylated at 100 ℃ for 2.5 h. GC-MS analysis was performed using an Agilent 6890A-5975C gas chromatograph. The scanning range (m/z) was 50-350.

2.3.8 Nuclear magnetic resonance spectroscopy (NMR)

The dried AS-3 was dissolved in D_2O and prepared to 40 mg/mL. ^{1}D-NMR (^{1}H NMR, ^{13}C NMR) and ^{2}D-NMR (COSY, NOESY, HMBC and HSQC) were recorded by applying a Bruker AVANCE NEO 500M spectrometer system.

2.4 Prebiotic characterization of almond polysaccharide AS-3

2.4.1 Preparation of human fecal filtrate

Four volunteers (2 males and 2 females, aged 20 - 30 years, without gastrointestinal diseases and antibiotics for at least 3 months) were screened, and fresh feces from the four volunteers were mixed in equal parts in an anaerobic table, and then saline solution was added immediately to make a 20 % mixture (w/w). The mixture was homogenized for 2 min, and the filtrate was collected after aseptic filtration and set aside. The experimental protocol was approved by the Ethics Committee of Shenyang Agricultural University (approval number 2023060101). All volunteers were able

to comply with the study procedures and provided written informed consent before the start of the experiment.

2.4.2 Preparation of fermentation medium

The 1 L of medium was formulated about the previous method with minor modifications(Bianchi et al., 2011), specifically, containing 3 g casein, 2 g yeast extract, 2 g peptone, 2 g $NaHCO_3$, with the addition of 0.5 g bovine bile salt, 0.5 g cysteine hydrochloride, 0.1 g NaCl, 0.04 g KH_2PO_4, 0.04 g K_2HPO_4, 0.01 g $CaCl_2$, and 0.01 g $MgSO_4 \cdot H_2O$. In addition, 20 mg of hemoglobin, 2 mL of Tween-80, 1 mL of bladed azurite solution (0.025 %, w/v), and 10 μL of vitamin K_1 were added, and finally, autoclave sterilization was performed at 121 °C for 20 min.

2.4.3 In vitro fermentation

The in vitro fermentation mixture system was modified from the previous method(Ma et al., 2021). In brief, 100 mg of AS-3 was added to each anaerobic tube in an anaerobic station, and the positive control group used inulin instead of AS-3. All the anaerobic tubes were placed in an incubator at 37 °C. The fermentation broth was collected at different time points (0, 6, 12, 24 and 48 h), and the supernatant and precipitate were stored in a -80 °C refrigerator.

2.4.4 Determination of fermentation broth pH

At the time points of 0, 6, 12, 24, and 48 h, respectively, 3 mL of fermentation broth was taken from the anaerobic fermentation tubes of each group, put in an ice-water bath to cool down for 10 min, and centrifuged at 10,000 r/min for 5 min, then the change of pH of the fermentation broths of each group was determined.

2.4.5 Determination of SCFAs in fermentation broth

SCFAs were obtained by mixing 500 μL of fermentation broth with 500 μL of ether, ultrasonication for 5 min, vigorous shaking for 2 min to prepare the sample solution, and centrifugation at 10000 r/min. SCFAs were determined by GC-MS using an HP-FFAP column (25 m × 200 μm × 0.3 μm): 1 μL of the sample was injected into the sample at an initial temperature of 80 ℃, then heated to 140 ℃ at a rate of 7.5 ℃/min, and then heated to 200 ℃ at a rate of 15 ℃/min, and kept for 3 min. The initial temperature was 80 ℃, then heated to 140 ℃ at a rate of 7.5 ℃/min, and then heated to 200 ℃ at a rate of 15 ℃/min, and kept for 3 min.

2.4.6 16S rRNA and bioinformatics analysis

Fecal fermentation broth from 24 and 48 h of fermentation was taken by centrifugation at 10,000 rpm/min for 10 min, and the precipitate was collected with bacterial DNA extracted. The V3-V4 highly variable region of bacterial 16S rRNA was amplified by PCR

using universal primers 338F (sequence 5′-ACTCCTACGGGGGAGGCAGCA -3′) and 806R (sequence 5′-GGACTACHVGGGGTWTCTAAT -3′). Next, the products were analyzed by 2 % agarose gel electrophoresis and the target DNA fragments were recovered using the AxyPrep DNA Gel Recovery Kit. With the help of Quant-iT PicoGreen dsDNA Assay Kit and quantified on a Microplate reader. Finally, the processed DNA samples were sequenced and analyzed on the MiSeq platform.

2.5 Statistical analysis

All experimental data were expressed based on the mean and standard deviation (Mean ± SD) of three independent experiments to ensure the accuracy and reliability of the results. ANOVA and Duncan tests were performed on the data using SPSS 29.0 software, and $P < 0.05$ was considered significant.

3. Results

3.1 Isolation and purification of AS-3

As shown in Fig. 1B, the crude polysaccharide ASDF was chromatographically separated on a DEAE-52 cellulose column to obtain four fractions. After comparison, the fraction with the highest yield was selected for further purification using a Sephadex G-100 dextran gel column. The elution chromatogram after secondary

purification by Sephadex G-100 was shown in Fig. 1C, which presented a single peak. In addition, the yield of AS-3 was 13.5 % relative to the almond crude polysaccharide ASDF. The total sugar content of AS-3 was 97.2 ± 0.4, with only a small amount of glucuronic acid (2.2 ± 0.1).

3.2 UV spectral analysis

According to the UV spectrogram shown in Fig. 1D, it can be observed that AS-3 did not show characteristic absorption peaks at 260 nm and 280 nm, which indicated that AS-3 did not contain protein and nucleic acid components.

3.3 Molecular weight and molecular configuration analysis

The molecular weight and chain conformation of AS-3 components were determined using the SEC-MALLS-RI system. The molar mass distribution was shown in Fig. 1E, where the refractive index signal (RI) curve could be seen to show a single symmetric peak, which indicated that AS-3 was homogeneous. Mw, Mn, and polydispersity index were presented in Table 1. The polydispersity index of AS-3 was closer to 1 than that of the AP-1 fraction of almond polysaccharides obtained by our previous hot-water leaching method(Peng et al., 2023), indicating that it is a moderately dispersed macromolecule with a more consistent internal molecular weight composition and better homogeneity. As shown in Fig. 1F, the molecular radius versus molar mass

correlation for AS-3 was a linear line with a negative slope. The negative slopes suggested that the molecular radius changes in the opposite direction to the molar mass and that the linear chains were not independent, but rather interconnected(J. H. Lee et al., 2009). Therefore, we hypothesize that AS-3 may exist in a mixed conformation.

Table 1 Absolute molecular weight result

Component name	Mw (kDa)	Mn (kDa)	Mz (kDa)	Mp (kDa)	Polydispersity index
AS-3	50.956	40.201	75.536	33.494	1.268

3.4 Monosaccharide composition analysis

The composition of AS-3 was composed of five monosaccharides, arabinose, galactose, rhamnose, glucose, and glucuronic acid, with a molar ratio of 47.72: 39.85: 6.62: 1.92: 3.89, as shown in Fig. 2A. Arabinose and galactose were the major monosaccharides in the AS-3 fractions. In addition, we found that its monosaccharide composition was like that of blueberry leaf polysaccharides (Hu et al., 2024), which have hypolipidemic and hypoglycemic activities, as well as polysaccharides from *Protaetia brevitarsis seulensis* (Olawuyi et al., 2025), which activate antiviral immunity. Therefore, we hypothesized that AS-3 is also a biologically active polysaccharide.

3.5 FT-IR analysis

The absorption peaks in the region of 3600-3200 cm^{-1} are characteristic peaks of sugars(L. Wang, Liu, et al., 2018). As shown

in Fig. 2B, a broad peak at 3435.78 cm^{-1} can be seen for AS-3, which is ascribed to the O-H stretching vibration. In addition, the absorption peak at 2927.96 cm^{-1} on the spectrogram reveals the telescopic vibration of C-H, while there is an absorption peak at 1073.81 cm^{-1} attributed to the stretching vibration of C-O(H. Zhang et al., 2021).

3.6 SEM analysis

As shown in Fig. 2C and 2D, at 500 Í magnification AS-3 has striped and rounded flakes appearing; at 5000 Í, AS-3 can be seen to be flaked and flattened rounded, and the flattened rounded surfaces are accompanied by obvious holes. Polysaccharide molecules can be arranged in an orderly manner under certain conditions through interactions such as hydrogen bonding and van der Waals forces to form sheet-like aggregates (L. Wang et al., 2021). This lamellar morphology may be related to the linear or mildly branched structural characteristics of polysaccharide molecules (Y. Li et al., 2018). Moreover, the appearance of the oblate shape may be due to the flexibility of the polysaccharide molecules as well as the mutual attraction between the different regions, which makes them agglomerate into a more regular oblate shape to a certain extent. In addition, during the extraction of polysaccharides, different enzymes act on polysaccharides at different sites and to different extents. Certain enzymes may act preferentially on specific sites of polysaccharide molecular aggregates, resulting in cleavage of glycosidic bonds and cross-

links between molecules, thus leaving pores on the surface of the oblate aggregates (Panwar et al., 2024).

3.7 Triple-stranded helix structure analysis

Congo red can form complexes with polysaccharides having a triple-stranded helical chain conformation, and the maximum absorption wavelength (λ_{max}) of such complexes is red-shifted compared to that of the Congo red solution alone. The λ_{max} value of this complex shows a decreasing trend as the NaOH concentration gradually increases (Zhang et al., 2021). As shown in Fig. 2E, the λ_{max} of the AS-3 mixed solution is lower than that of Congo red when the NaOH concentration is 0. At low NaOH concentration (0.1 M), the λ_{max} of the AS-3 mixed solution undergoes a red shift, followed by a blue shift with increasing base concentration. Therefore, we speculate that AS-3 has a triple-stranded helical structure. Numerous studies have shown that the monosaccharide composition, molecular weight, and tertiary conformation of polysaccharides are the key factors affecting their antioxidant, anti-inflammatory, and immunomodulatory activities. Such as *Hylocereus undatus* polysaccharide with a high content of uronic acid, medium molecular weight and triple-helix structure had higher antioxidant activity and immunomodulatory activity than the other two fractions (C. Li et al., 2023), as well as ginger polysaccharide with triple-helix structure had immunomodulatory activity (X. Yang et al., 2021). Combined, these examples suggest that the triple-stranded helical structure, among other key features of the

polysaccharide, may play a crucial role in conferring a variety of beneficial biological activities, necessitating further investigation of the structure and associated functions of AS-3 to understand its potential applications fully.

3.8 Methylation and GC-MS analysis

How polysaccharides are linked, and the content of sugar residues are key elements in determining their structure and function(Fernandes & Coimbra, 2023). AS-3 was analyzed using methylation and GC-MS methods, and the results were shown in Table 2, with a total of six linkages, t-Ara(f), 5-Ara(f), 2,4-Rha(p), 3-Gal(p), 6-Gal(p), 3,6-Gal(p), and the relative molar ratios of 30.06: 17.85: 2.1: 18.38: 4.8: 26.82. In addition, small amounts of rhamnose, glucose, and glucuronic acid were not detected compared to the results of the monosaccharide composition, which may be due to their low levels.

It has been shown that the linkage mode of polysaccharides shapes the unique spatial conformation of polysaccharides, and the content of sugar residues can directly affect the physicochemical properties and biological activities of polysaccharides, for instance, the anti-inflammatory activity of polysaccharides from *Ashwagandha* with β-(1→3, 1→6) glucose residues and triple-helix structure is higher than that of polysaccharides with β-(1→3, 1→4) glucose residues (Jen et al., 2021). Similarly, for the five subfractions of asparagus skin polysaccharides with 4-α-d-GalpA as the major sugar residue, the higher the content of 4-α-d-GalpA

sugar residue the stronger the immunological activity (N. Wang et al., 2021). In this study, we identified multiple glycosidic linkages, including 3-Gal(p), 6-Gal(p), 3,6-Gal(p), and t-Ara(f). This corresponds to structurally similar pectin polysaccharides found in the pollen of *Typha angustifolia L.*, which have been demonstrated to alleviate oleic acid-induced hepatic steatosis by inhibiting lipid accumulation and oxidative stress(Xu et al., 2023). This further supports the hypothesis that structural features of AS-3—such as the type and linkage of sugar residues—may exert a significant influence on its biological activity, particularly in terms of immunomodulation and metabolic protection.

Table 2 The results of methylation analysis of AS-3

Name	Linkage types	Methylation products	Major mass fragments (m/z)	RT (min)	MW	Molar ratio (%)
AS-3	t-Ara(f)	1,4-di-O-acetyl-2,3,5-tri-O-methyl arabinitol	71,87,102,118,129,145,161	6.048	279	30.06
	5-Ara(f)	1,4,5-tri-O-acetyl-2,3-di-O-methyl arabinitol	87,102,118,129,162,189	10.695 0	307	17.85
	2,4-Rha(p)	1,2,4,5-tetra-O-acetyl-6-deoxy-3-O-methyl rhamnitol	88,101,117,130,143,190,203	12.410	349	2.10
	3-Gal(p)	1,3,5-tri-O-acetyl-2,4,6-tri-O-methyl galactitol	87,101,118,129,161,202,234	12.856	351	18.38
	6-Gal(p)	1,5,6-tri-O-acetyl-2,3,4-tri-O-methyl galactitol	87,99,102,118,129,162,189,233	15.490	351	4.80
	3,6-Gal(p)	1,3,5,6-tetra-O-acetyl-2,4-di-O-methyl galactitol	87,101,118,129,160,189,234	18.960	379	26.82

3.9 NMR analysis

The NMR signals of the major sugar residues of AS-3 were attributed as follows: Sugar residue A, with a heterophyid signal

4.98/107.35 ppm (H1/C1), suggesting that residue A may be an arabinose residue of α-configuration (Fig. 3A) (Fig. 3B). Further, in the COSY profile (Fig. 3C), H2 (4.02 ppm) of residue A was confirmed based on the cross-peak 4.98/4.02 ppm, H3 (3.83 ppm) of residue A was clarified based on the cross-peak 4.02/3.83 ppm, H4 (3.62 ppm) of residue A was determined with the help of the cross-peak 3.83/3.62 ppm, H5 (3.71, 3.74 ppm) of residue A was identified with the help of cross peaks 3.62/3.71, 3.74 ppm and the above was attributed to the chemical shift of H on the sugar ring. After that, the chemical shifts of C on this sugar ring were attributed to HSQC signals, and the C1 chemical shift of residue A was 107.35 ppm, the C2 chemical shift of residue A was 80.82 ppm, the C3 chemical shift of residue A was 76.5 ppm, the C4 chemical shift of residue A was 80.04 ppm, and the C5 chemical shift was 61.02 ppm, in which the C1 chemical shift is biased towards the low field, indicating that the residue is substituted at the O-1 position of the sugar ring. Combining the results of methylation analysis with literature reports (Zhang et al., 2020; B. H. Wang et al., 2019), it can be inferred that the sugar residue A may be α-L-Araf-(1→.

Sugar residue B, the heterophyid signal 5.04/107.02 ppm (H1/C1) indicated that residue B could be an α-configuration galactose residue. In the COSY profile (Fig. 3C), H2 (4.05 ppm) of residue B was identified based on the cross peak 5.04/4.05 ppm, H3 (4.01 ppm) of residue B based on the cross peak 4.05/4.01 ppm, and H4 (3.92 ppm) of residue B based on the cross peak 4.01/3.92 ppm. H5 (3.65 ppm) of residue B was determined based on the cross peak 3.92/3.65 ppm, and H6 (3.72,3.83 ppm) of residue B was determined based on the cross peak 3.65/3.72, 3.83 ppm, and up

to this point the chemical shifts of the hydrogens on the sugar ring were attributed. Subsequently, the chemical shift of C on this sugar ring was assigned by the HSQC signal (Fig. 3E). The C1 chemical shift of residue B was 107.02 ppm, the C2 chemical shift of residue B was 69.31 ppm, the C3 chemical shift of residue B was 83.79 ppm, the C4 chemical shift of residue B was δ68.91 ppm, the C5 chemical shift of residue B was 70 ppm, and the C6 chemical shift of residue B was 66.43 ppm, where the C1, C3, and C6 chemical shifts were moved to the lower field, which indicated that the residue was substituted at the O-1, O-3, and O-6 positions of the sugar ring. In combination with the results of methylation analysis and literature reports (B. H. Wang et al., 2019; Zeng et al., 2020), it can be inferred that the sugar residue B may be →3,6)-α-D-Galp-(1→.

Regarding sugar residue C, the hetero-head signal 4.42/103.09 ppm (H1/C1) suggested that residue C might be a β-configuration galactose residue. In the COSY spectrum (Fig. 3C), H2 (3.31 ppm) of residue C was determined based on the cross peak 4.42/3.31 ppm, H3 (3.94 ppm) of residue C was identified based on the cross peak 3.31/3.94 ppm, H4 (3.54 ppm) of residue C was established based on the cross peak 3.94/3.54 ppm, H5 (3.82 ppm) of residue C was determined based on the cross peak 3.54 /3.82 ppm, and H6 (3.6,3.67 ppm) of residue C was determined from the cross-peak 3.82/3.6,3.67 ppm, which led to the attribution of the chemical shift of hydrogen on the sugar ring. Then, the chemical shift of C on this sugar ring was attributed to the HSQC signal (Fig. 3E). The chemical shift of C1 of residue C was 103.09 ppm, C2 of residue C was 71.87 ppm, C3 of residue C was 83.92 ppm, C4 of residue C was 69.82 ppm, C5 of residue C was 73.23 ppm, and C6 of residue C was 61.2

ppm, where the C1 and C3 were shifted to the lower field, which indicated that the residue was substituted at the O-1, O-3 position of the sugar ring. Considering the results of methylation analysis and literature reports (B. H. Wang et al., 2019;Ding et al., 2018), it can be inferred that the sugar residue C may be →3)-β-D-Galp-(1→. The attribution results of each sugar residue displacement are shown in Table 3.

Table 3 Chemical shifts for the residues of AS-3.

Code	Glycosyl residues	Chemical shifts(ppm)					
		H1/C1	H2/C2	H3/C3	H4/C4	H5/C5	H6/C6
A	α-L-Ara*f*-(1→	4.98	4.02	3.83	3.62	3.71,3.74	/
		107.35	80.82	76.5	80.04	61.02	/
B	→3,6)-α-D-Gal*p*-(1→	5.04	4.05	4.01	3.92	3.65	3.72,3.83
		107.02	69.31	83.79	68.91	70	66.43
C	→3)-β-D-Gal*p*-(1→	4.42	3.31	3.94	3.54	3.82	3.6,3.67
		103.09	71.87	83.92	69.82	73.23	61.2
D	→5)-α-L-Ara*f*-(1→	5.13	4.11	4.18	4.2	4.12,3.82	/
		109.19	82.18	79.02	81.21	68.41	/

Based on the chemical shifts of ^{13}C and ^{1}H of each sugar residue in the sample, combined with the HMBC spectra (Fig. 3F), we analyzed the structure and the connections present in the polysaccharides: H1 of sugar residue A has a cross-peak 4.98/66.43 ppm with C6 of sugar residue B, H1 of sugar residue B has a cross-peak 5.04/83.79 ppm with C3 of sugar residue B, H1 of sugar residue B H1 of sugar residue C exists cross peak δ5.04/83.92 ppm with C3 of sugar residue C, and H1 of sugar residue D exists cross peak 5.13/83.79 ppm with C3 of sugar residue B. The NOESY spectra (Fig. 3D) were further combined to determine and speculate on the linkage order of the residues in the polysaccharide. There were cross peaks 4.98/3.72 ppm and

4.98/3.83 ppm between H1 of sugar residue A and H6 of sugar residue B. Cross peaks 5.04/4.01 ppm existed between H1 of sugar residue B and H3 of sugar residue B. The H1 of sugar residue B has a cross peak 5.04/3.94 ppm with the H3 of sugar residue C, while the H1 of sugar residue C has cross peaks 4.42/4.12 ppm and 4.42/3.82 ppm with the H5 of sugar residue D, and the H1 of sugar residue D has a cross peak 5.13/4.01 ppm with the H3 of sugar residue B.

Therefore, combining the ^{1}D and ^{2}D NMR information as well as the analysis of methylation results, it was deduced that AS-3 is mainly composed of →3,6)-α-D-Galp-(1→, →3)-β-D-Galp-(1→, and →5)-α-L-Araf-(1→ interconnected to form the main chain, whereas the branched chain was composed of α-L-Araf-(1→ connected to the O-6 position of →3,6) -α-D-Galp-(1→.

The presence and linkage position of side chains are crucial structural factors influencing biological activity. Previous studies have demonstrated a positive correlation between the branching degree of polysaccharides and antioxidant activity: within a certain molecular weight range, a higher number of side chains enhances radical scavenging efficiency (Fernandes & Coimbra, 2023). The side chains of AS-3 are attached to the O-6 position of the main chain via α-L-Araf-(1→. This branching pattern may confer favorable spatial exposure, enabling terminal residues to readily interact with free radicals or bind to receptor molecules. In addition, the ratio and arrangement of →3,6)-α-D-Galp-(1→ and →3)-β-D-Galp-(1→ units in the main chain may significantly influence the physical properties and biological activity of the polysaccharide (R. Chen et al., 2022).

Specifically, the →3,6)-α-D-Galp-(1→ unit serves as the branching point for side chains. An excessively high proportion of this unit may result in a higher branching density along the main chain, leading to increased rigidity. Conversely, if the →3)-β-D-Galp-(1→ unit predominates, the chain may exhibit greater linearity and flexibility. This balance between rigidity and flexibility is crucial for the affinity of polysaccharides toward free radicals or receptor binding. The biological activity of polysaccharides is also related to whether their sugar chains can bind to cell surface receptors. It has been demonstrated that arabinogalactan structures in plant polysaccharides often exhibit potent immunostimulatory activity, capable of activating macrophages, dendritic cells, and other immune cells (Shen et al., 2024). Therefore, the Galp and Araf residues in AS-3 may be recognized by sugar-recognition receptors on the surface of immune cells, thereby regulating cytokine expression and immune activation responses.

3.10 Changes in pH of fermentation broth

Acetic acid, butyric acid and other acidic substances produced by polysaccharide fermentation can inhibit harmful bacteria and promote the growth of beneficial bacteria, with the role of regulating immunity and maintaining the integrity of the intestinal barrier (Blaak et al., 2020). In this study, the pH value of the fermentation broth was measured at each time point of polysaccharide fermentation to reflect the fermentation process of polysaccharides and the production rate of acidic products. As shown in Fig. 4A, the initial pH

of the fermentation medium of the blank group was weakly alkaline. With the prolongation of fermentation time, the pH of the fermentation broth of the blank group was always close to 7, indicating that the microorganisms did not have intense metabolic activities in the absence of additional polysaccharides. When the fermentation time was increased from 12 h to 24 h, the pH of the fermentation broth of the inulin group slightly increased, while the pH of the AS-3 group was continuously decreasing, which may be due to that some alkali-producing bacteria in the inulin group started to be active at this fermentation time. In addition, the pH of the fermentation broth of the AS-3 group was lower than that of the inulin group when the fermentation time reached 24 h and 48 h.

AS-3, as a novel polysaccharide, may be more difficult to degrade in terms of its monosaccharide composition, glycosidic bond type, or branching structure than that of inulin (β-2,1-fructose), leading to sustained fermentation. This slow-release property may slow down the metabolic rate of acid-producing bacteria, thus avoiding a premature shift of the colony to protein fermentation (Sarbini et al., 2011). The low pH environment can improve glucose metabolism and reduce intestinal permeability by activating FFAR2 receptors in intestinal epithelial cells, promoting GLP-1 secretion(Ducastel et al., 2020) and enhancing tight junction protein expression(Song et al., 2022). Meanwhile, the acidic intestinal environment could attenuate the inflammatory response by inhibiting the TLR4/NF-κB pathway(Y. S. Lee & Olefsky, 2021).

3.11 Changes in the production of SCFAs during in vitro fermentation

SCFAs are a subset of fatty acids that are produced by the gut microbiota during fermentation of partially contrast, certain gut bacteria, such as *Bifidobacterium* and *Enterococcus*, have been noted to metabolize galactose fully and non-digestible polysaccharides and play an important role in the maintenance of health and disease (Tan et al., 2014). In Fig. 4B, it can be found that the total amount of SCFAs in all groups except the BLK group increased with fermentation time, which coincided with the trend of decreasing pH of the fermentation broth with the increase of fermentation time, suggesting that the carbon source was well utilized. The concentration of the total SCFAs in the AS-3 group increased rapidly from 12 h of fermentation, and during the fermentation period from 12 h to 24 h, AS-3's bioavailability was significantly better than that of inulin ($P < 0.001$).

The concentrations of SCFA in each group at different time points are shown in Table 4, with the most apparent changes in the concentrations of acetic acid, propionic acid, and n-butyric acid. Acetic acid can eventually generate acetyl coenzyme A through a series of metabolic reactions in the body, thus entering the tricarboxylic acid cycle, which is an important pathway for energy production in human cells (Hallows et al., 2006). During the process of fermentation from 0h to 24h, there was no significant difference ($P > 0.05$) in the acetic acid production of the AS-3 group compared to the INL group, whereas the maximum change in the acetic acid concentration of the AS-3 group occurred from 24h to 48h. The

physiological functions of propionic acid are also not to be ignored, as it can regulate immune cells and slow down the loss of vascular endothelial function and regulate intestinal inflammation by up-regulating the expression of ICAM-1 and E-selectin, which plays an important role in maintaining the health of the body and the stability of the internal environment (M. Wang et al., 2019). After 48 h of fermentation, the amount of change in propionic acid in the AS-3 group was approximately 5.4 times that of the BLK group and 1.2 times that of the INL group. It has been found that subjects with slow-turning constipation (STC) have lower levels of acetic and propionic acids with a significant negative correlation between the levels of these two acids and the severity of constipation (Q. Chen et al., 2024). Therefore, we hypothesized that AS-3 may have a biological function in relieving constipation. Butyrate can mediate the enhancement of the mechanical integrity of the intestinal mucosal barrier by promoting the up-regulation of the gene expression of the tight junction protein Claudin-1 and the closed small-band protein ZO-1, or by modulating the dynamic reorganization of their cell membrane localization (Kumar et al., 2015). The amount of change in n-butyric acid in the AS-3 group was significantly higher than that in the INL group when the fermentation time reached 12 h ($P < 0.05$), but the trend was reversed after 48 h of fermentation. This indicated that AS-3 had an advantage in the production of n-butyric acid in the pre-fermentation period, but the stability might not be as good as that of inulin. In the field of liver disease research, the treatment of acute liver injury (AILI) has been a key focus. One study found that the combined use of N-acetylcysteine (NAC) and butyrate significantly improved the

survival of AILI mice and revealed that butyrate induced both mitochondrial autophagy and Nrf2 antioxidant response through the AMPK-ULK1-p62 signaling pathway, thereby alleviating AILI-induced iron death(C.-J. Yang et al., 2024).

In the past, it has been shown that acetate accounts for the highest percentage of total SCFAs, thus the trend of acetate is like the trend of total SCFAs (C. Fu et al., 2023). Interestingly, we found AS-3 has a stronger ability to regulate butyric acid than acetic acid. This might be a unique metabolic regulatory mechanism that may be related to the targeted regulatory effects of AS-3 on specific intestinal flora, such as proliferating butyric acid-producing flora, which leads to a significant increase in butyric acid concentration. Therefore, we will next conduct in-depth studies on AS-3-regulated intestinal flora to reveal its mechanism of action.

Table 4 Changes in SCFAs concentration produced at different time points during fecal fermentation

Sample	Fermentation time (h)	SCFAs (mmol/L)						
		Acetic acid	Propionic acid	i-Butyric acid	n-Butyric acid	i-Valeric acid	n-Valeric acid	Caproic acid
BLK	0	$1.09 \pm 0.02^{C,a}$	$0.75 \pm 0.24^{B,a}$	$0.22 \pm 0.07^{C,a}$	$0.312 \pm 0.12^{C,b}$	$0.07 \pm 0.05^{B,b}$	$0.12 \pm 0.01^{AB,a}$	$1.7 \pm 0.22^{A,a}$
	6	$1.09 \pm 0.04^{B,a}$	$0.44 \pm 0.11^{C,a}$	$0.06 \pm 0.03^{C,b}$	$0.74 \pm 0.13^{B,b}$	$0.26 \pm 0.17^{A,b}$	$0.23 \pm 0.08^{A,a}$	$0.28 \pm 0.06^{C,b}$
	12	$1.13 \pm 0.03^{B,b}$	$0.4 \pm 0.02^{C,b}$	$0.22 \pm 0.04^{C,b}$	$0.65 \pm 0.17^{B,c}$	$0.06 \pm 0.02^{B,b}$	$0.14 \pm 0.07^{AB,a}$	$0.33 \pm 0.16^{BC,a}$
	24	$1.1 \pm 0.02^{B,b}$	$0.32 \pm 0.15^{C,c}$	$0.58 \pm 0.21^{B,a}$	$0.67 \pm 0.19^{B,b}$	$0.07 \pm 0.03^{B,a}$	$0.06 \pm 0.01^{B,b}$	ND
	48	$1.39 \pm 0.23^{A,c}$	$1.39 \pm 0.09^{A,c}$	$1.42 \pm 0.11^{A,a}$	$3.16 \pm 0.02^{A,c}$	$0.12 \pm 0.04^{AB,a}$	$0.22 \pm 0.07^{A,a}$	$0.6 \pm 0.15^{B,a}$
AS-3	0	$1.21 \pm 0.13^{D,a}$	$0.22 \pm 0.04^{D,b}$	$0.25 \pm 0.03^{AB,a}$	$1.68 \pm 0.08^{E,a}$	$0.12 \pm 0.07^{B,b}$	$0.07 \pm 0.03^{C,a}$	$0.67 \pm 0.1^{A,b}$
	6	$1.51 \pm 0.6^{D,a}$	$0.33 \pm 0.03^{D,ab}$	$0.36 \pm 0.1^{A,a}$	$6.2 \pm 0.28^{D,a}$	$0.27 \pm 0.02^{A,b}$	$0.09 \pm 0.02^{C,a}$	$0.23 \pm 0.05^{B,b}$
	12	$2.54 \pm 0.38^{C,a}$	$2.56 \pm 0.09^{C,a}$	$0.36 \pm 0.03^{A,a}$	$12.07 \pm 0.78^{C,a}$	$0.13 \pm 0.02^{B,a}$	$1.27 \pm 0.04^{A,a}$	ND
	24	$3.78 \pm 0.19^{B,a}$	$5.29 \pm 0.13^{B,a}$	$0.16 \pm 0.03^{B,b}$	$19.3 \pm 0.43^{B,a}$	$0.06 \pm 0.03^{BC,a}$	$0.28 \pm 0.12^{B,a}$	ND
	48	$8.36 \pm 0.55^{A,b}$	$7.23 \pm 0.11^{A,a}$	ND	$25.95 \pm 1.11^{A,b}$	$0.03 \pm 0.01^{C,b}$	$0.14 \pm 0.04^{C,a}$	$0.33 \pm 0.06^{B,b}$
INL	0	$1.24 \pm 0.15^{C,a}$	$0.19 \pm 0.07^{C,b}$	$0.47 \pm 0.34^{A,a}$	$2.13 \pm 0.52^{D,a}$	$0.76 \pm 0.04^{A,a}$	$0.17 \pm 0.04^{A,a}$	$1.53 \pm 0.29^{A,a}$
	6	$1.47 \pm 0.37^{C,a}$	$0.22 \pm 0.03^{C,b}$	$0.46 \pm 0.07^{A,a}$	$6.17 \pm 1.48^{C,a}$	$0.71 \pm 0.07^{A,a}$	$0.14 \pm 0.09^{A,a}$	$0.71 \pm 0.23^{B,a}$
	12	$3.71 \pm 0.94^{B,a}$	$0.39 \pm 0.06^{C,b}$	$0.26 \pm 0.03^{A,b}$	$7.3 \pm 1.45^{C,b}$	$0.11 \pm 0.04^{B,ab}$	$0.08 \pm 0.02^{A,b}$	ND
	24	$3.43 \pm 0.41^{BC,a}$	$1.88 \pm 0.37^{B,b}$	ND	$19.67 \pm 1.6^{B,a}$	$0.09 \pm 0.02^{B,a}$	$0.14 \pm 0.07^{A,ab}$	ND

48	11.25 ± 2.36^{A,a}	6.02 ± 0.32^{A,b}	ND	32.11 ± 2.14^{A,a}	0.04 ± 0.01^{B,b}	0.11 ± 0.05^{A,a}	0.65 ± 0.06^{B,a}

Note: Upper-case letters indicate significant differences (P < 0.05) between the same group at different time points, and lower-case letters indicate significant differences (P < 0.05) between different groups at the same time point. BLK: no carbon source group; AS-3: AS-3 treated group; INL: inulin treated group; ND: not detected

3.12 Impact on microbial diversity

3.12.1 Alpha diversity analysis

Polysaccharides can influence the alpha diversity of microbial communities, either increasing their diversity by promoting microbial growth and providing diverse ecological niches, or inhibiting some microbes by altering environmental conditions, leading to a decrease in diversity (So et al., 2018). To investigate the effects of the almond polysaccharide AS-3 on the production of healthy human intestinal flora, 16S rRNA sequencing of the microorganisms was carried out at 24 and 48 hours of fermentation, respectively. As can be seen from Fig. 4C, the sparse curves of each group gradually flattened out with the increase of the subsampling depth. It indicates that the current depth of sequencing provides good coverage of the microbial species in the samples. By comparing and analyzing the results of 24h and 48h fermentation of the AS-3 group under the condition of maintaining the same sequencing depth, it can be found that the species richness is relatively higher at 24h fermentation. This result proves that the 24h treatment time has a more significant effect on the enhancement of microbial diversity compared with 48h.

Further comparison also revealed that the microbial diversity of the AS group was consistently higher than that of the INL group at all times of fermentation. The above results suggested that the intervention time of almond polysaccharide AS-3 played a key role in the enhancement of intestinal flora diversity, and its enhancement effect was better than that of inulin. This may be since within 24 h, AS-3 provided a more suitable growth substrate for beneficial intestinal microorganisms, which promoted the proliferation and diversification of microorganisms. However, with the extension of time to 48h, the growth of microorganisms may be limited due to the accumulation of metabolites or nutrient depletion, resulting in a decrease in diversity. The unique chemical structure and properties of AS-3 may allow it to be better utilized by gut microbes compared to inulin, thus more effectively contributing to microbial community development and diversity enhancement. It has been shown that arabinose intake enriches specific beneficial bacteria, enhancing microbial richness and gut health (Hosseini et al., 2023). In contrast, certain gut bacteria, such as *Bifidobacterium* and *Enterococcus*, have been noted to metabolize galactose from pectin and increase butyrate concentration, which is consistent with our previous findings that AS-3 significantly enhances butyrate concentration (T. Zhao et al., 2025).

Fig. 4D showed the abundance rank curve, which demonstrated the abundance distribution of OTUs (operational taxonomic units) in different samples. The curve for the AS group is flatter than that for the INL group, indicating that the microbial abundance distribution in the samples of the AS group is relatively more uniform. Compared with the AS24 group, the distance between the curves of the AS48

group and the BLK group is greater, which implies that the almond polysaccharide has different effects on the microbial community structure under different treatment times. Regarding the effect of intervention time on gut microorganisms, previous studies have shown that highland hull-less barley significantly changed the structure of the gut microbial community in rats at different intervention times (Xia et al., 2024). It can be shown that the time factor is very critical for the regulation of intestinal flora. Therefore, when applying almond polysaccharides to intervene in the intestinal flora, the time should also be precisely controlled to achieve the ideal effect of flora regulation.

In Fig. 4E, the four different coverage indices are shown between the different sample groups. In terms of the CHAO1 index, which is used to assess species richness, the Shannon index, which represents species richness and species evenness, and the Simpson index, which measures species diversity, the AS24 group was significantly higher than the AS48 group ($P < 0.05$), indicating that the structure of the gut microbial community was richer and more balanced at 24 h of fermentation of AS-3 than that at 48 h. Meanwhile, the index values of the AS group were higher than those of the positive control INL group at both 24 h and 48 h. This indicates that the structure of the gut microbial community at 24 h of AS-3 fermentation was more abundant and balanced than that at 48 h. The conclusion is consistent with the results of the sparse curve and the abundance rank curve.

In terms of the Goods coverage index, the index of the INL group was higher and significantly different from all other treatment groups,

indicating better sequencing coverage compared to the other intervention groups. Similarly, the coverage of AS48 was significantly better than that of AS24, but there was no significant difference between INL24 and INL48 (p > 0.05), and these differences may be related to the different intervention treatments.

3.12.2 Beta diversity analysis

Principal Coordinate Analysis (PCoA) is used to explore microbial community structure, which is based on a distance algorithm that maps differences in the composition of sample microbial communities to point distances in a multidimensional space, where sample spacing is inversely related to community similarity (Koc et al., 2022). As shown in Fig. 4F, PCo1 explained 42.6% and PCo2 explained 19.1% of the variance in the data, which means that these dimensions can reflect the differences in the composition of microbial communities among the samples to a certain extent. Observation of the distribution of sample points within the AS and INL groups showed that the sample points were more concentrated within the groups, suggesting that the microbial community structure within the groups was more similar. In addition, there was no overlap in the distribution areas of the sample sites of the AS and INL groups, indicating that the microbial community structures of the two groups differed significantly. It is worth noting that the distance between the AS group and the BLK group gradually increased when the fermentation time was extended from 24h to 48h, which implies that the difference in microbial community structure between the AS group and the BLK group further

increased over time. This may be because the fermentation process is dynamic, and prolonged fermentation will lead to substrate depletion and metabolite accumulation, which will change the ecological niche of the microbial community (B. Liu et al., 2023). For instance, the acidic metabolites produced in the early stage of fermentation may inhibit the growth of acid-intolerant microorganisms and create an advantage for acid-tolerant microorganisms, which in turn drives a significant change in the community structure at 48h relative to 24h. The difference with the BLK group is more prominent (Strain et al., 2020).

The Venn diagram in Fig. 4G presented the common and unique status of OTUs among different sample groups. In terms of the number of unique OTUs, the order of BLK48＞BLK24＞AS24＞AS48＞INL48＞INL24 is shown. Meanwhile, the number of OTUs shared by the six groups is only 56. The high number of unique OTUs indicates the uniqueness of the microbial community of the group, while the high number of common OTUs indicates the high similarity of the microbial community composition among the groups (D. Sun et al., 2021). These results suggest that there are some commonalities and significant differences in microbial community composition among the groups, and the differences in the number of unique OTUs imply that different treatments or temporal factors play different roles in shaping the microbial community structure.

3.13 Effects on microbial species

The effect of AS-3 on microbial gate levels is shown in Fig. 5A. After 24 h of fermentation, the AS-3 group promoted the proliferation of *Firmicutes* and inhibited *Bacteroidetes*, *Actinobacteria* and *Proteobacteria* compared to the BLK group, suggesting that AS-3 was able to alter the growth dynamics of different phylum in the intestinal flora at the early stage of fermentation, and exerted a directional regulation of the bacterial community structure. The results showed that AS-3 was able to change the growth status of different phylum in the intestinal flora at the early stage of fermentation. When the fermentation time reached 48h, the abundance of *Bacteroidetes* and *Firmicutes* was higher in the AS-3 group than in the other two groups, and the abundance of *Proteobacteria* was always at a lower level. Previous studies have shown that an increased *Firmicutes/Bacteroidetes* ratio and reduced *Proteobacteria* abundance are closely associated with improved intestinal barrier integrity and reduced colitis severity (Z. Li et al., 2023) (J. Liu et al., 2023). Considering that AS-3 shares similar arabinogalactan-rich structural features with known anti-inflammatory polysaccharides (M. Li et al., 2025) (C. Cao et al., 2021), it is reasonable to infer that AS-3 may exert a protective effect against colitis by modulating gut microbiota composition and inflammatory responses, although further in vivo validation is needed.

The changes in the intestinal flora of the INL group were different from those of the AS-3 group. The abundance of *Proteobacteria* in the INL24 and INL48 groups was as high as 68.55% and 38.38%, whereas the abundance in the AS-3 group was consistently less than 27%, suggesting that AS-3 was more effective than INL in

suppressing the number of potentially pathogenic bacteria. It has also been shown that most of the propionate is produced by *Firmicutes* and *Bacteroidetes* through the succinate pathway (J. Wu et al., 2023), which is consistent with our findings that the AS-3 group produced more propionate than all other groups.

The *Firmicutes/Bacteroidetes* (F/B) ratio in the AS-3 group markedly decreased from 9.18 at 24 h to 2.04 at 48 h, indicating that the microbial composition tended toward a more balanced and stable state. In contrast, the INL group showed an increasing F/B ratio during fermentation, while the BLK group exhibited a passive decline from 4.95 to 1.33 due to spontaneous microbial succession. Although both AS-3 and BLK groups displayed downward trends, the pronounced reduction in the AS-3 group—from an initially high and imbalanced level to a physiologically moderate range—was significantly different and more favorable than that of the BLK group (P = 0.045), indicating that AS-3 actively modulated the gut microbial community in a distinct and more controlled manner rather than reflecting a natural fermentation process.

Beyond the modulation of the F/B ratio, AS-3 exhibited additional prebiotic features through the selective enrichment of beneficial SCFA-producing taxa such as *Clostridiaceae*, while concurrently suppressing potential pathogens like *Enterobacteriaceae*. SCFAs play crucial roles in maintaining intestinal barrier integrity, modulating inflammatory responses, and reducing oxidative stress. These microbial and metabolic shifts align with the known pharmacological activities of almond, which have been reported to

exhibit anti-inflammatory and antioxidant properties (Rajaram et al., 2023), promote the growth of beneficial bacteria and SCFA production (Rajaram et al., 2023) (Creedon et al., 2022) , and exhibit certain hepatoprotective effects (Humaira Jamshed et al., 2020). Therefore, the prebiotic function of AS-3 may extend beyond phylum-level balance to encompass a broader enhancement of gut microbial functionality and host metabolic health.

At the family level, the effect of AS-3 on the bacterial flora has been dynamic and new changes have been produced over time. As shown in Figure 5B, compared with the BLK group, the relative abundance of *Clostridiaceae* was significantly higher in the AS-3 group after 24 h of fermentation, and the relative abundance of *Enterobacteriaceae*, *Peptostreptococcaceae*, *Bacteroidaceae* and *Coriobacteriaceae* was significantly decreased. After 48 h of fermentation, the relative abundance of *Enterobacteriaceae* and *Coriobacteriaceae* was still decreasing in the AS-3 group, while the relative abundance of *Clostridiaceae*, *Porphyromonadaceae* and *Ruminococcaceae* was increased. Increased *Clostridiaceae* abundance is linked to several health benefits, especially those derived from dietary supplements rich in probiotics, prebiotics, or other bioactive compounds. Recent studies have shown that tea polyphenols can beneficially modulate the gut microbiota, enhancing *Clostridiaceae* abundance and reducing the occurrence of preneoplastic lesions(Z. Yang et al., 2025). It has also been shown that *Clostridiaceae* and *Ruminococcaceae* are important producers of butyrate, which is consistent with our (Ladeira Bernardes et al., 2025).

At the genus level (Fig. 5C), we found that [*Clostridium*], *Bacteroides*, *Dialister*, and *Parabacteroides*, which were enriched in the AS-3 group, had low abundance in the INL group, both at 24h and 48h of fermentation, consistent with the findings of our previous study that the Alpha diversity of the AP-3 group was significantly higher than that of the INL group ($P < 0.05$). The primary metabolite of [*Clostridium*] is butyric acid, which regulates the expression of genes involved in lipid metabolism and inflammation, affecting health outcomes in models of immunosuppression and metabolic syndrome(H. Fu et al., 2025). *Bacteroides* have been shown to play an important role in disease amelioration and immunomodulation, significantly improving metabolic function and contributing to host immune balance(N. Liu et al., 2025; L. Li et al., 2023; E. Chen et al., 2025), but also actively participating in host immunomodulation through the AHR-Nrf2 pathway, enhancing epithelial barrier function and reducing inflammation(Luo et al., 2025). However, the role of *Bacteroides* in colitis is controversial. Several studies have shown that increased *Bacteroides* abundance is associated with the production of pro-inflammatory cytokines in the context of inflammatory bowel disease (Livingston et al., 2025; J. Li et al., 2025; Xiong et al., 2025). In contrast, other studies have shown that *Bacteroides* contribute to immune regulation, potentially suppressing excessive inflammatory responses and preventing diseases such as colitis and colorectal cancer (Z. Chen et al., 2025). For instance, it has been studied that polysaccharides extracted from black goji berries can modulate *Bacteroides* abundance and reduce inflammatory markers in DSS-induced colitis. There are also certain *Bacteroides* that produce butyric acid with anti-inflammatory

properties that help maintain the integrity of the intestinal barrier (Lonescu et al., 2025). Thus, *Bacteroides* can modulate host immune responses that are pro-inflammatory or inhibitory, depending on the specific species and environmental context.

There have also been studies suggesting that yoghurt, inulin, and appropriate exercise increase the relative abundance of *Dialister* in the gut (Lkhagva et al., 2021), that lower levels of *Dialister* may be associated with depression(Parletta et al., 2019)。An increased abundance of *Dialister* has been associated with shifts in other gut genera in multiple human cohorts, including positive co-occurrence with *Dorea* and inverse relationships with certain beneficial taxa such as *Bifidobacterium* in specific disease contexts (Gryaznova et al., 2024)(Vuralli et al., 2024). These associations suggest that changes in *Dialister* may contribute to, or at least mark, the altered abundance of *Bacteroides*, *Bifidobacterium*, *Adlercreutzia* and *Dorea* observed in the AS-3 group, although direct causal interactions remain to be established. *Parabacteroides* are closely related to host health, possessing the ability to improve metabolic syndrome, inflammatory bowel disease and obesity (Leibovitzh et al., 2025). It can mitigate inflammatory responses and maintain immune system homeostasis by promoting the expression of the anti-inflammatory cytokine IL-10 (Guo et al., 2024). Another study has shown that polysaccharides from plant sources can promote beneficial flora, including *Parabacteroides*, improve gut health and reduce T2DM-related intestinal disease (Y. Zhao et al., 2025).

The modulatory effect of AS-3 on gut microbiota may be closely related to its structural characteristics. AS-3 has a moderate molecular weight (50.956 kDa) and is composed mainly of arabinose and galactose, with minor amounts of rhamnose, glucose, and glucuronic acid, indicating an arabinogalactan-rich structure. Polysaccharides rich in arabinose and galactose are known to be highly fermentable by members of *Clostridiaceae*, and *Ruminococcaceae*, which are capable of degrading complex plant glycans and producing SCFAs, particularly butyrate(C. Cao et al., 2021)(Gao et al., 2025). The presence of branched linkages such as →3,6)-α-D-Galp-(1→ and →5)-α-L-Araf-(1→ also facilitates microbial enzymatic accessibility and selective fermentation by beneficial anaerobes(Silva et al., 2025), while limiting rapid degradation by opportunistic taxa like *Proteobacteria*(Y. Sun et al., 2021). These structural features may therefore underlie the observed enrichment of butyrate-producing genera (e.g., *Clostridium*, *Ruminococcus*) and the concurrent suppression of potentially pathogenic groups (e.g., *Enterobacteriaceae*) following AS-3 fermentation. Together, the unique monosaccharide composition, moderate molecular weight, and branched arabinogalactan backbone of AS-3 likely contribute to its prebiotic and anti-inflammatory effects by promoting SCFA production and maintaining microbial homeostasis.

3.14 Species composition heatmap with LEfSe analysis

Differential bacteria in the AS-3 group were analyzed by heat map and LEfSe for 24h and 48h of fermentation. Fig. 5D showed

the relative abundance of the top 20 genus, with the heat bar colors ranging from low (blue) to high (red) to reflect the change in abundance. The relative abundance of the beneficial genera *Clostridium, Collinsella, Blautia* and [*Ruminococcus*] increased and the abundance of the harmful genera *Enterococcus* and *Shigella* decreased in the AS-3 group after 24 h of fermentation compared to the INL group. *Clostridium* has been shown to metabolize butyric acid and to have immunomodulatory effects (Bakky et al., 2025), while *Collinsella* and [*Ruminococcus*] specialize in the degradation of cellulose (Carlson et al., 2017; Chassard et al., 2012), contributing to the maintenance of intestinal homeostasis. *Blautia* can promote normal peristalsis and digestion in the intestinal tract and reduce the incidence of constipation (J. Zhou et al., 2024). *Enterococcus* and *Shigella* are both potentially pathogenic genera of enteric bacteria. *Enterococcus*, as a conditionally pathogenic bacterium, often triggers infections when the body's immunity is low or the flora is imbalanced (Krawczyk et al., 2021), while *Shigella* is a typical pathogen that directly attacks the colonic mucosa and causes bacillary dysentery, both of which can threaten the host's health and exacerbate the risk of intestinal diseases in case of an imbalance in the intestinal microecology (Ducarmon et al., 2019).

When the fermentation time was extended to 48 h, the AS-3 group differed from the other groups by boosting the relative abundance of *Dialister*, *Dorea*, *Oscillospira*, *Parabacteroides*, *Sutterella*, and [*Eubacterium*], while INL differed by being able to cause a significant increase in the relative abundance of *Bifidobacterium* and *Lactobacillus*. *Oscillospira* is closely linked to the metabolic health of the host, affecting fat storage and

metabolism (Konikoff & Gophna, 2016), and *Eubacterium* also plays an important role in the regulation of obesity-related metabolism. Its increased abundance may have an ameliorative effect on obesity by affecting bile acid metabolism(Zhi et al., 2025). Alterations in gut microbiota composition have been closely linked to the pathophysiology of anxiety and depressive disorders. Recent systematic analyses have reported that the abundance of *Sutterella* is significantly reduced in individuals with anxiety and major depressive disorder, implying that this genus may exert anti-inflammatory and neuroprotective effects via the gut–brain axis(Y. Cao et al., 2025)(L. Liu et al., 2023)). In the present study, the observed elevation of *Sutterella* following AS-3 treatment may therefore indicate a microbiota-mediated mechanism that contributes to the attenuation of intestinal inflammation and the restoration of gut–brain homeostasis. Nevertheless, further mechanistic and in vivo studies are required to confirm the potential antidepressant and neuroimmune regulatory roles of AS-3.

The results of linear discriminant analysis (LDA) scoring thresholds greater than 4 are shown in Fig. 5E and 5F. After 24 h of fermentation in the BLK group, there were 4 categories of biomarkers, including 3 genera. There were 7 classes of biomarkers after 48 h of fermentation, including 3 classes of genera. This indicates that the bacterial population of the BLK group changed little during the fermentation process, probably lacked dominant genera that could proliferate continuously, and the microecological regulation ability was weak. Under the intervention of AS-3, the intestinal flora changed significantly. A total of 5 classes of

biomarkers, including *Clostridium*, were identified after 24 h of fermentation of AS-3, suggesting that it may initially regulate the intestinal microecology by promoting the proliferation of specific genera, such as *Clostridium* etc. A total of 10 classes of biomarkers were recognized by AS-3 after 48 h of the fermentation process, which covered 1 class of phylum and 3 classes of genus-level classification, including *Bacteroidetes*, *Dialister*, *Parabacteroides* and *Dorea*. It has been suggested that *Bacteroidetes* are associated with metabolic health, whereas *Dialister* and *Parabacteroides* may be involved in carbohydrate metabolism, and *Dorea* is associated with inflammatory regulation, suggesting that AS-3 may work synergistically through multiple bacteria to optimize gut function further (Senthilkumar & Arumugam, 2025; Farmakioti et al., 2025). In contrast, the number of biomarkers was lower in the INL group, with a total of 5 types of biomarkers, including 1 type of phylum and 1 type of genus, *Proteobacteria* and *Shigella*, at 24 h of fermentation. In addition, at 48 h of fermentation, there were a total of 5 types of biomarkers, including 1 type of phylum and 1 type of genus, *Actinobacteria*. Among them, *Proteobacteria* was associated with intestinal inflammation (Y. Zhang et al., 2024). However, although *Bifidobacterium* is a well-known probiotic, an isolated increase in *Bifidobacterium* may not be sufficient to counteract the expansion of proinflammatory taxa. Although inulin is generally considered beneficial for gut health, emerging evidence suggests that excessive or unbalanced intake may lead to microbial dysbiosis and exacerbate intestinal inflammation in susceptible hosts. In particular, high inulin consumption has been associated with altered bile acid metabolism and type 2 inflammatory responses at mucosal surfaces

(Arifuzzaman et al., 2022), as well as with succinate accumulation and inflammation-associated colonic tumorigenesis due to microbial dysregulation (Tian et al., 2023). Therefore, the intervention in the INL group might carry a potential risk of flora imbalance or mild inflammatory responses.

3.15 Spearman correlation analysis between gut flora and short-chain fatty acids

SCFAs are critical for gut integrity, inflammatory regulation, and metabolic processes, and their interactions with the gut microbiota provide ideas for dietary interventions targeting gut health and related chronic diseases(Throat & Bhattacharya, 2025). Thus, we used Spearman correlation analysis to explore the relationship between gut flora and SCFAs. Correlation analysis between SCFAs and intestinal flora was performed using Spearman. As shown in Fig. 5G, the relative abundance of *Shigella* was significantly negatively correlated ($P < 0.05$) with acetic acid and significantly positively correlated ($P < 0.05$) with the relative abundance of *Clostridium*, *Dialister* and *Dorea* at 24 h of fermentation in the AS-3 group. Propionic acid and n-valeric acid content were also significantly positively correlated ($P < 0.05$) with the relative abundance of *Clostridium*, while n-butyric acid was significantly negatively correlated ($P < 0.05$) with the relative abundance of *Clostridium* and *Bacteroides*. In addition, for 48 h of fermentation (Fig. 5H), the flora positively correlated with acetic acid content was consistent with 24 h. Unlike the AS-3 group fermented for 48 h, *Clostridium*, *Dialister*, *Parabacteroides* and *Collinsella* were positively correlated with

propionic acid in AS-3 at 24 h, which may be related to the depletion of metabolized substrates by the colony or intergeneric competition. Moreover, the amount of n-butyric acid and the abundance of *Collinsella* in the AS-3 group were always significantly positively correlated ($P < 0.05$).

Regarding the relationship between the composition of the flora and the change in the content of total SCFAs, there was a significant positive correlation between the change in the content of total SCFAs and the relative abundance of *Clostridium* ($P < 0.05$), however, the opposite was true for the relative abundance of *Dorea*. Like the results for the AS-3 group fermented for 24 h, the abundance of *Clostridium* and *Dorea* in the AS-3 group after 48 h of fermentation remained significantly positively correlated ($P < 0.05$) with the content of total SCFAs.

Overall, AS-3 intervention synergistically elevated the levels of SCFAs by promoting the proliferation of acid-producing genera such as *Clostridium* and *Dialister*, and indirectly enhanced metabolic functions by inhibiting pro-inflammatory bacteria such as *Shigella*. The dynamic association between the flora and SCFAs was time-dependent(Yokota et al., 2025), with rapid acid-producing bacteria dominating in the early stage and shifting to the synergistic effect of complex substrate-metabolizing bacteria in the later stage. The results provide evidence for the metabolic level of the prebiotic mechanism of AS-3, but further validation of the functions of key genera in vivo models is needed to advance its application in metabolic disease intervention.

4. Conclusion

AS-3, an almond polysaccharide isolated from almonds, has good prebiotic effects. The main chain consists of →3,6)-α-D-Gal-(1→, →3)-β-D-Gal-(1→ and →5)-α-L-Araf-(1→, and the branched chain consists of α-L-Araf-(1→ attached to the O-6 position of →3,6)-α-D-Gal-(1→. Moreover, AS-3 exhibits the potential to improve intestinal microecology by increasing the production of SCFAs, improving the structure of the intestinal flora, increasing the abundance of beneficial bacteria, and decreasing the abundance of harmful bacteria. In view of the close association between intestinal flora and metabolic diseases, we can focus on the application of AS-3 in metabolic diseases in the future and open a new pathway for natural polysaccharides in metabolic disease prevention and treatment.

CRediT authorship contribution statement

Yanqi Peng: Writing – original draft, Validation, Methodology, Formal analysis, Data curation, Conceptualization. **Ji Wu:** Writing – review & editing, Funding acquisition, Project administration, Data curation. **Mingyue Ma:** Visualization, Software, Methodology. **Yuzhen Pi:** Conceptualization, Methodology, Supervision, Formal analysis. **Xiqing Yue:** Investigation, Methodology, Supervision, Project administration, Funding acquisition, Conceptualization. **Yanyu Peng:** Writing – review & editing, Supervision, Project administration, Investigation, Funding acquisition, Conceptualization.

Declaration of competing interest

The authors have declared that they have no known competing financial interests or personal relationships that could have appeared to influence the work reported in this paper.

Acknowledgment

This study was supported by the Liaoning Province Revitalization Talents Program (NO. XLYC1902083); the Doctoral Start-up Foundation of Liaoning Province, China (2022-BS-340); the Science and Technology Research Project of Department of Education of Liaoning Province (JYTZD2023145), the Science and Technology Key Research Project of Liaoning Province (2024JH2/102500059) and Research Project on Integrated Traditional Chinese and Western Medicine for Chronic Disease Management (CXZH2024134).

Ethical approval

The experimental animal protocol complied with ARRIVE guidelines and was carried out according to the National Research Council's Guide for the Care and Use of Laboratory Animals (8th edition). The experimental protocol was approved by the Ethics Committee of Shenyang Agricultural University (approval number 2023060101). All volunteers were able to comply with the study procedures and provided written informed consent before the start of the experiment.

Data availability

Data will be made available on request.

Reference

Arifuzzaman, M., Won, T. H., Li, T.-T., Yano, H., Digumarthi, S., Heras, A. F., Zhang, W., Parkhurst, C. N., Kashyap, S., Jin, W.-B., Putzel, G. G., Tsou, A. M., Chu, C., Wei, Q., Grier, A., Longman, R., Sonnenberg, G., Scherl, E., Sockolow, R., … Artis, D. (2022). Inulin fibre promotes microbiota-derived bile acids and type 2 inflammation. *Nature*, *611*(7936), 578–584. https://doi.org/10.1038/s41586-022-05380-y

Bakky, Md. A. H., Tran, N. T., Zhang, M., Wang, S., Zhang, Y., & Li, S. (2025). Synergistic effects of butyrate-producing bacteria (Clostridium senegalense I5 or Paraclostridium benzoelyticum G5) and Gracilaria lemaneiformis-originated polysaccharides on the growth and immunity of rabbitfish. *International Journal of Biological Macromolecules*, *291*, 138683. https://doi.org/10.1016/j.ijbiomac.2024.138683

Beaver, L. M., Leonard, S. W., Uesugi, S. L., Wong, C. P., Lytle, L.-M., Vasudevan, A., Papenhausen, E. M., Jupudi, Y., Bella, D., Bobe, G., Traber, M. G., & Ho, E. (2025). Beneficial changes in total cholesterol, LDL-C, biomarkers of intestinal inflammation, and vitamin E status in adults with metabolic syndrome consuming almonds as snack foods: a randomized controlled clinical trial. *Nutrition Research*, *139*, 50–65. https://doi.org/10.1016/j.nutres.2025.04.011

Bianchi, F., Dall'Asta, M., Del Rio, D., Mangia, A., Musci, M., & Scazzina, F. (2011). Development of a headspace solid-phase microextraction gas chromatography-mass spectrometric method for the determination of short-chain fatty acids from intestinal fermentation. *Food Chemistry*, *129*(1), 200–205. https://doi.org/10.1016/j.foodchem.2011.04.022

Blaak, E. E., Canfora, E. E., Theis, S., Frost, G., Groen, A. K., Mithieux, G., Nauta, A., Scott, K., Stahl, B., van Harsselaar, J., van Tol, R., Vaughan, E. E., & Verbeke, K. (2020). Short chain fatty acids in human gut and metabolic health. In *Beneficial*

Microbes (Vol. 11, Issue 5, pp. 411–455). Wageningen Academic Publishers. https://doi.org/10.3920/BM2020.0057

Cao, C., Zhu, B., Liu, Z., Wang, X., Ai, C., Gong, G., Hu, M., Huang, L., & Song, S. (2021). An arabinogalactan from *Lycium barbarum* attenuates DSS-induced chronic colitis in C57BL/6J mice associated with the modulation of intestinal barrier function and gut microbiota. *Food & Function*, *12*(20), 9829–9843. https://doi.org/10.1039/D1FO01200B

Cao, Y., Cheng, Y., Pan, W., Diao, J., Sun, L., & Meng, M. (2025). Gut microbiota variations in depression and anxiety: a systematic review. *BMC Psychiatry*, *25*(1), 443. https://doi.org/10.1186/s12888-025-06871-8

Carlson, J., Erickson, J., Hess, J., Gould, T., & Slavin, J. (2017). Prebiotic Dietary Fiber and Gut Health: Comparing the in Vitro Fermentations of Beta-Glucan, Inulin and Xylooligosaccharide. *Nutrients*, *9*(12), 1361. https://doi.org/10.3390/nu9121361

Chassard, Christophe, Delmas, Eve, Robert, , Céline, Lawson, P. A., & Bernalier-Donadille, A. (2012). Ruminococcus champanellensis sp. nov., a cellulose-degrading bacterium from human gut microbiota. *International Journal of Systematic and Evolutionary Microbiology*, *62*(1), 138–143. https://doi.org/10.1099/ijs.0.027375-0

Chen, E., Ajami, N. J., White, D. L., Liu, Y., Gurwara, S., Hoffman, K., Graham, D. Y., El-Serag, H. B., Petrosino, J. F., & Jiao, L. (2025). Dairy Consumption and the Colonic Mucosa-Associated Gut Microbiota in Humans—A Preliminary Investigation. *Nutrients*, *17*(3), 567. https://doi.org/10.3390/nu17030567

Chen, Q., Chen, D., Gao, X., Jiang, Y., Yu, T., Jiang, L., & Tang, Y. (2024). Association between fecal short-chain fatty acid levels and constipation severity in subjects with slow transit constipation. *European Journal of Gastroenterology & Hepatology*, *36*(4), 394–403. https://doi.org/10.1097/MEG.0000000000002734

Chen, R., Xu, J., Wu, W., Wen, Y., Lu, S., El-Seedi, H. R., & Zhao, C. (2022). Structure–immunomodulatory activity relationships of dietary polysaccharides. *Current Research in Food Science*, *5*, 1330–1341. https://doi.org/10.1016/j.crfs.2022.08.016

Chen, Z., Zhang, Z., Nie, B. N., Huang, W., Zhu, Y., Zhang, L., Xu, M., Wang, M., Yuan, C., Liu, N., Wang, X., Tian, J., Ba, Q., & Wang, Z. (2025). Temporal network analysis of gut microbiota

unveils aging trajectories associated with colon cancer. *MSystems*. https://doi.org/10.1128/msystems.01188-24

Creedon, A. C., Dimidi, E., Hung, E. S., Rossi, M., Probert, C., Grassby, T., Miguens-Blanco, J., Marchesi, J. R., Scott, S. M., Berry, S. E., & Whelan, K. (2022). The impact of almonds and almond processing on gastrointestinal physiology, luminal microbiology, and gastrointestinal symptoms: a randomized controlled trial and mastication study. *The American Journal of Clinical Nutrition*, *116*(6), 1790–1804. https://doi.org/10.1093/ajcn/nqac265

Ding, H. H., Qian, K., Goff, H. D., Wang, Q., & Cui, S. W. (2018). Structural and conformational characterization of arabinoxylans from flaxseed mucilage. *Food Chemistry*, *254*, 266–271. https://doi.org/10.1016/j.foodchem.2018.01.159

Ducarmon, Q. R., Zwittink, R. D., Hornung, B. V. H., van Schaik, W., Young, V. B., & Kuijper, E. J. (2019). Gut Microbiota and Colonization Resistance against Bacterial Enteric Infection. *Microbiology and Molecular Biology Reviews*, *83*(3). https://doi.org/10.1128/MMBR.00007-19

Ducastel, S., Touche, V., Trabelsi, M.-S., Boulinguiez, A., Butruille, L., Nawrot, M., Peschard, S., Chávez-Talavera, O., Dorchies, E., Vallez, E., Annicotte, J.-S., Lancel, S., Briand, O., Bantubungi, K., Caron, S., Bindels, L. B., Delzenne, N. M., Tailleux, A., Staels, B., & Lestavel, S. (2020). The nuclear receptor FXR inhibits Glucagon-Like Peptide-1 secretion in response to microbiota-derived Short-Chain Fatty Acids. *Scientific Reports*, *10*(1), 174. https://doi.org/10.1038/s41598-019-56743-x

Fabiano, G. A., Oliveira, R. P. S., Rodrigues, S., Santos, B. N., Venema, K., & Antunes, A. E. C. (2025). Evidence of synbiotic potential of oat beverage enriched with inulin and fermented by L. rhamnosus LR B in a dynamic in vitro model of human colon. *Food Research International*, *211*, 116489. https://doi.org/10.1016/j.foodres.2025.116489

Farmakioti, I., Stylianopoulou, E., Siskos, N., Karagianni, E., Kandylas, D., Vasileiou, A. R., Fragkiskatou, F., Somalou, P., Tsaroucha, A., Ypsilantis, P., Panas, P., Kourkoutas, Y., Skavdis, G., & Grigoriou, M. E. (2025). Enhancing Gut Microbiome and Metabolic Health in Mice Through Administration of Presumptive Probiotic Strain Lactiplantibacillus pentosus PE11. *Nutrients*, *17*(3), 442. https://doi.org/10.3390/nu17030442

Fernandes, P. A. R., & Coimbra, M. A. (2023). The antioxidant activity of polysaccharides: A structure-function relationship overview. *Carbohydrate Polymers*, *314*, 120965. https://doi.org/10.1016/j.carbpol.2023.120965

Fu, C., Ye, K., Ma, S., Du, H., Chen, S., Liu, D., Ma, G., & Xiao, H. (2023). Simulated gastrointestinal digestion and gut microbiota fermentation of polysaccharides from Agaricus bisporus. *Food Chemistry*, *418*. https://doi.org/10.1016/j.foodchem.2023.135849

Fu, H., Li, X., Guo, X., Yang, D., Nan, C., Cheng, J., Du, H., Shen, M., & Wang, J. (2025). Consolidated bioprocessing of cassava starch into butyric acid and butanol by engineered Clostridium butyricum SCUT 620. *Bioresource Technology*, *417*, 131870. https://doi.org/10.1016/j.biortech.2024.131870

Gao, G., Cai, L., Fan, Y., Aroche Ginarte, R., Li, Y., Sun, W., Jiang, X., Li, X., & Pi, Y. (2025). Effects of Different Hemicellulose Components on Fermentation Kinetics and Microbial Composition in Fecal Inoculum from Suckling Piglets *In Vit ro*. *ACS Omega*, *10*(9), 9120–9131. https://doi.org/10.1021/acsomega.4c08848

Gryaznova, M., Smirnova, Y., Burakova, I., Morozova, P., Lagutina, S., Chizhkov, P., Korneeva, O., & Syromyatnikov, M. (2024). Fecal Microbiota Characteristics in Constipation-Predominant and Mixed-Type Irritable Bowel Syndrome. *Microorganisms*, *12*(7). https://doi.org/10.3390/microorganisms12071414

Guo, Z., Xiao, S., Chen, G., Zhong, S., Zhong, H., Sun, S., Chen, P., Tang, X., Yang, H., Jia, Y., Yin, Z., Huang, L., & Wang, Y. (2024). Disruption of the gut microbiota-inflammation-brain axis in unmedicated bipolar disorder II depression. *Translational Psychiatry*, *14*(1), 495. https://doi.org/10.1038/s41398-024-03207-0

Hallows, W. C., Lee, S., & Denu, J. M. (2006). Sirtuins deacetylate and activate mammalian acetyl-CoA synthetases. *Proceedings of the National Academy of Sciences*, *103*(27), 10230–10235. https://doi.org/10.1073/pnas.0604392103

Hosseini, A., Barlow, G. M., Leite, G., Rashid, M., Parodi, G., Wang, J., Morales, W., Weitsman, S., Rezaie, A., Pimentel, M., & Mathur, R. (2023). Consuming artificial sweeteners may alter the structure and function of duodenal microbial communities. *IScience*, *26*(12), 108530. https://doi.org/10.1016/j.isci.2023.108530

Hu, Y., Wang, D., Zhang, Y., Chen, S., Yang, X., Zhu, R., & Wang, C. (2024). A novel polysaccharide from blueberry leaves: Extraction, structural characterization, hypolipidemic and hypoglycaemic potentials. *Food Chemistry*, *460*, 140493. https://doi.org/10.1016/j.foodchem.2024.140493

Hui, H., Wang, Z., Zhao, X., Xu, L., Yin, L., Wang, F., Qu, L., & Peng, J. (2024). Gut microbiome-based thiamine metabolism contributes to the protective effect of one acidic polysaccharide from Selaginella uncinata (Desv.) Spring against inflammatory bowel disease. *Journal of Pharmaceutical Analysis*, *14*(2), 177–195. https://doi.org/10.1016/j.jpha.2023.08.003

Humaira Jamshed, Jamshed Arslan, Fatehali Tipoo Sultan, Hasan Salman Siddiqi, Muhammad Qasim, Anwar-ul-Hassan Gilani, & Admin. (2020). Almond protects the liver in coronary artery disease – a randomized controlled clinical trial. *Journal of the Pakistan Medical Association*, 1–15. https://doi.org/10.47391/JPMA.198

Ionescu, V. A., Diaconu, C. C., Gheorghe, G., Mihai, M.-M., Diaconu, C. C., Bostan, M., & Bleotu, C. (2025). Gut Microbiota and Colorectal Cancer: A Balance Between Risk and Protection. *International Journal of Molecular Sciences*, *26*(8), 3733. https://doi.org/10.3390/ijms26083733

Jen, C.-I., Su, C.-H., Lai, M.-N., & Ng, L.-T. (2021). Comparative anti-inflammatory characterization of selected fungal and plant water soluble polysaccharides. *Food Science and Technology Research*, *27*(3), 453–462. https://doi.org/10.3136/fstr.27.453

Ji, X., Peng, B., Ding, H., Cui, B., Nie, H., & Yan, Y. (2023). Purification, Structure and Biological Activity of Pumpkin Polysaccharides: A Review. *Food Reviews International*, *39*(1), 307–319. https://doi.org/10.1080/87559129.2021.1904973

Koc, F., Sugrue, I., Murphy, K., Renzetti, S., Noort, M., Ross, R. P., & Stanton, C. (2022). The microbiome modulating potential of superheated steam (SHS) treatment of dietary fibres. *Innovative Food Science & Emerging Technologies*, *80*, 103082. https://doi.org/10.1016/j.ifset.2022.103082

Konikoff, T., & Gophna, U. (2016). Oscillospira: a Central, Enigmatic Component of the Human Gut Microbiota. *Trends in Microbiology*, *24*(7), 523–524. https://doi.org/10.1016/j.tim.2016.02.015

Krawczyk, B., Wityk, P., Gałęcka, M., & Michalik, M. (2021). The Many Faces of Enterococcus spp.—Commensal, Probiotic and

Opportunistic Pathogen. *Microorganisms*, *9*(9), 1900. https://doi.org/10.3390/microorganisms9091900

Kumar, A., Alrefai, W. A., Borthakur, A., & Dudeja, P. K. (2015). *Lactobacillus acidophilus* counteracts enteropathogenic *E. coli* -induced inhibition of butyrate uptake in intestinal epithelial cells. *American Journal of Physiology-Gastrointestinal and Liver Physiology*, *309*(7), G602–G607. https://doi.org/10.1152/ajpgi.00186.2015

Ladeira Bernardes, A., Albuquerque Pereira, M. de F., Xisto Campos, I., Ávila, L., dos Santos Cruz, B. C., Duarte Villas Mishima, M., Maciel dos Santos Dias, M., de Oliveira Mendes, T. A., & Gouveia Peluzio, M. do C. (2025). Oral intake of Hibiscus sabdariffa L. increased c-Myc and caspase-3 gene expression and altered microbial population in colon of BALB/c mice induced to preneoplastic lesions. *European Journal of Nutrition*, *64*(3), 109. https://doi.org/10.1007/s00394-025-03622-z

Lee, J. H., Han, J. A., & Lim, S. T. (2009). Effect of pH on aqueous structure of maize starches analyzed by HPSEC-MALLS-RI system. *Food Hydrocolloids*, *23*(7), 1935–1939. https://doi.org/10.1016/j.foodhyd.2008.12.007

Lee, Y. S., & Olefsky, J. (2021). Chronic tissue inflammation and metabolic disease. *Genes & Development*, *35*(5–6), 307–328. https://doi.org/10.1101/gad.346312.120

Leibovitzh, H., Fliss Isakov, N., Werner, L., Thurm, T., Hirsch, A., Cohen, N. A., & Maharshak, N. (2025). A Mushroom Based Prebiotic Supplement Pilot Study Among Patients with Crohn's Disease. *Journal of Dietary Supplements*, 1–14. https://doi.org/10.1080/19390211.2025.2498127

Li, C., Zhang, Y., Zhao, C., & Fu, X. (2023). Physicochemical characterization, antioxidative and immunoregulatory activity of polysaccharides from the flower of Hylocereus undatus (Haw.) Britton et Rose. *International Journal of Biological Macromolecules*, *251*, 126408. https://doi.org/10.1016/j.ijbiomac.2023.126408

Li, J., Xu, J., Hu, J., Xu, H., Guo, X., Zhang, Y., Xu, J., Huang, C., Nie, Y., & Zhou, Y. (2025). PPARγ/β/δ Agonists Can Ameliorate Dextran Sodium Sulfate–Induced Colitis and Modulate Gut Microbiota. *Journal of Gastroenterology and Hepatology*. https://doi.org/10.1111/jgh.16929

Li, L., Yan, S., Liu, S., Wang, P., Li, W., Yi, Y., & Qin, S. (2023). In-depth insight into correlations between gut microbiota and

dietary fiber elucidates a dietary causal relationship with host health. *Food Research International*, *172*, 113133. https://doi.org/10.1016/j.foodres.2023.113133

Li, M., Wu, H., Li, Y., Wang, X., Xu, N., Ge, H., Gao, X., Jiang, X., Jiang, Z., Xie, Z., Wang, Y., Li, D., & Wang, H. (2025). A Novel Acidic Polysaccharide from *Eurotium cristatum* -Fermented Dark Tea: Structural Characterization and Dual Modulation of Adipose Inflammation-Gut Microbiota Axis. *Journal of Agricultural and Food Chemistry*, *73*(39), 24753–24768. https://doi.org/10.1021/acs.jafc.5c07225

Li, Y., Chen, J., Cao, L., Li, L., Wang, F., Liao, Z., Chen, J., Wu, S., & Zhang, L. (2018). Characterization of a novel polysaccharide isolated from Phyllanthus emblica L. and analysis of its antioxidant activities. *Journal of Food Science and Technology*, *55*(7), 2758–2764. https://doi.org/10.1007/s13197-018-3199-6

Li, Z., Wang, X., Deng, X., Song, J., Yang, T., Liao, Y., Gong, G., Huang, L., Lu, Y., & Wang, Z. (2023). High-sensitivity qualitative and quantitative analysis of human, bovine and goat milk glycosphingolipids using HILIC-MS/MS with internal standards. *Carbohydrate Polymers*, *312*, 120795. https://doi.org/10.1016/j.carbpol.2023.120795

Lian, J., Zhang, Y., Dong, K., Shi, J., Zhang, F., Shan, G., Liu, P., Wang, N., & Jia, T. (2025). Enhanced oral bioavailability of two Cistanche polysaccharides in acteoside: an in-depth analysis of intestinal flora, short-chain fatty acids, and pharmacokinetic regulation. *Frontiers in Nutrition*, *12*. https://doi.org/10.3389/fnut.2025.1509734

Liu, B., Zhang, Z., Liu, X., Hu, W., & Wu, W. (2023). Gastrointestinal Fermentable Polysaccharide Is Beneficial in Alleviating Loperamide-Induced Constipation in Mice. *Nutrients*, *15*(20), 4364. https://doi.org/10.3390/nu15204364

Liu, C., Miao, Y., Zhao, J., Yang, S., Cheng, S., Zhou, W., Guo, W., & Li, A. (2025). In vitro simulated digestion of different heat treatments sweet potato polysaccharides and effects on human intestinal flora. *Food Chemistry*, *463*, 141190. https://doi.org/10.1016/j.foodchem.2024.141190

Liu, J., Che, Y., Cai, K., Zhao, B., Qiao, L., Pan, Y., Yang, K., & Liu, W. (2023). miR-136 Regulates the Proliferation and Adipogenic Differentiation of Adipose-Derived Stromal Vascular Fractions by Targeting HSD17B12. *International*

Journal of Molecular Sciences, *24*(19), 14892. https://doi.org/10.3390/ijms241914892

Liu, L., Wang, H., Chen, X., Zhang, Y., Zhang, H., & Xie, P. (2023). Gut microbiota and its metabolites in depression: from pathogenesis to treatment. *EBioMedicine*, *90*, 104527. https://doi.org/10.1016/j.ebiom.2023.104527

Liu, N., Dai, S., Fan, X., Li, B., Chen, M., Gong, P., & Chen, X. (2025). In vitro fermentation of Auricularia auricula polysaccharides and their regulation of human gut microbiota and metabolism. *International Journal of Biological Macromolecules*, *306*, 141714. https://doi.org/10.1016/j.ijbiomac.2025.141714

Livingston, D. B. H., Sweet, A., Chowdary, M., Demissie, M. S., Rodrigue, A., Gedara, K. P., Kishore, L., Mahmoodianfard, S., & Power, K. A. (2025). Diet alters the effects of lipopolysaccharide on intestinal health and cecal microbiota composition in C57Bl/6 male mice. *The Journal of Nutritional Biochemistry*, 109951. https://doi.org/10.1016/j.jnutbio.2025.109951

Lkhagva, E., Chung, H.-J., Ahn, J.-S., & Hong, S.-T. (2021). Host Factors Affect the Gut Microbiome More Significantly than Diet Shift. *Microorganisms*, *9*(12), 2520. https://doi.org/10.3390/microorganisms9122520

Luo, Y., Lan, C., Ren, W., Wu, A., Yu, B., He, J., & Chen, D. (2025). Bacteroides thetaiotaomicron: A symbiotic ally against diarrhea along with modulation of gut microbial ecological networks via tryptophan metabolism and AHR-Nrf2 signaling. *Journal of Advanced Research*. https://doi.org/10.1016/j.jare.2025.04.016

Ma, Y., Jiang, S., & Zeng, M. (2021). In vitro simulated digestion and fermentation characteristics of polysaccharide from oyster (Crassostrea gigas), and its effects on the gut microbiota. *Food Research International*, *149*. https://doi.org/10.1016/j.foodres.2021.110646

Olawuyi, I. F., Heo, E., Jeong, M., Kim, J. H., Park, J.-J., Chae, J., Gwon, S., Do Lee, S., Kim, H., Ojulari, O. V., Song, Y.-B., Lee, B.-H., Gu, B. Bin, Kim, S. R., Lee, J. H., Lee, W., Hwang, J. S., Nam, J.-O., Hahn, D., & Byun, S. (2025). Acidic polysaccharide from the edible insect Protaetia brevitarsis seulensis activates antiviral immunity to suppress norovirus infection. *Carbohydrate Polymers*, *347*, 122587. https://doi.org/10.1016/j.carbpol.2024.122587

Özcan, M. M. (2023). A review on some properties of almond: ımpact of processing, fatty acids, polyphenols, nutrients, bioactive properties, and health aspects. *Journal of Food Science and Technology*, *60*(5), 1493–1504. https://doi.org/10.1007/s13197-022-05398-0

Panwar, D., Panesar, P. S., & Chopra, H. K. (2024). Green valorization approach of Citrus limetta peels by ultrasound-assisted enzymatic extraction for recovery of dietary fibers: Optimization, physicochemical, structural, functional, and thermal properties. *Biomass Conversion and Biorefinery*. https://doi.org/10.1007/s13399-024-05963-x

Paranthaman, S. (2025). Almond gum (Prunus amygdalus var. dulcis) as a multi-functional bio-polymer: A recent progress on properties, applications, and future opportunities. *International Journal of Biological Macromolecules*, *315*, 144511. https://doi.org/10.1016/j.ijbiomac.2025.144511

Parletta, N., Zarnowiecki, D., Cho, J., Wilson, A., Bogomolova, S., Villani, A., Itsiopoulos, C., Niyonsenga, T., Blunden, S., Meyer, B., Segal, L., Baune, B. T., & O'Dea, K. (2019). A Mediterranean-style dietary intervention supplemented with fish oil improves diet quality and mental health in people with depression: A randomized controlled trial (HELFIMED). *Nutritional Neuroscience*, *22*(7), 474–487. https://doi.org/10.1080/1028415X.2017.1411320

Peng, Y., Li, Y., Pi, Y., & Yue, X. (2024). Effects of almond (Armeniaca Sibirica L. Lam) polysaccharides on gut microbiota and anti-inflammatory effects on LPS-induced RAW264.7 cells. *International Journal of Biological Macromolecules*, *263*, 130098. https://doi.org/10.1016/j.ijbiomac.2024.130098

Peng, Y., Zhang, Z., Chen, W., Zhao, S., Pi, Y., & Yue, X. (2023). Structural characterization, α-glucosidase inhibitory activity and antioxidant activity of neutral polysaccharide from apricot (Armeniaca Sibirica L. Lam) kernels. *International Journal of Biological Macromolecules*, *238*. https://doi.org/10.1016/j.ijbiomac.2023.124109

Peng, Y., Zhu, J., Li, Y., Yue, X., & Peng, Y. (2024). Almond polysaccharides inhibit DSS-induced inflammatory response in ulcerative colitis mice through NF-κB pathway. *International Journal of Biological Macromolecules*, *281*, 136206. https://doi.org/10.1016/j.ijbiomac.2024.136206

Ragno, A., Imbesi, M., Gervasi, T., Smeriglio, A., Mandalari, G., Impellizzeri, D., & Trombetta, D. (2025). Impact of post-harvest

storage conditions on polyphenol composition and antioxidant activity in natural almonds. *Frontiers in Nutrition*, *12*. https://doi.org/10.3389/fnut.2025.1582434

Rajaram, S., Damasceno, N. R. T., Braga, R. A. M., Martinez, R., Kris-Etherton, P., & Sala-Vila, A. (2023). Effect of Nuts on Markers of Inflammation and Oxidative Stress: A Narrative Review. *Nutrients*, *15*(5), 1099. https://doi.org/10.3390/nu15051099

Sang, T., Guo, C., Guo, D., Wu, J., Wang, Y., Wang, Y., Chen, J., Chen, C., Wu, K., Na, K., Li, K., Fang, L., Guo, C., & Wang, X. (2021). Suppression of obesity and inflammation by polysaccharide from sporoderm-broken spore of Ganoderma lucidum via gut microbiota regulation. *Carbohydrate Polymers*, *256*, 117594. https://doi.org/10.1016/j.carbpol.2020.117594

Sarbini, S. R., Kolida, S., Naeye, T., Einerhand, A., Brison, Y., Remaud-Simeon, M., Monsan, P., Gibson, G. R., & Rastall, R. A. (2011). *In Vitro* Fermentation of Linear and α-1,2-Branched Dextrans by the Human Fecal Microbiota. *Applied and Environmental Microbiology*, *77*(15), 5307–5315. https://doi.org/10.1128/AEM.02568-10

Senthilkumar, H., & Arumugam, M. (2025). Gut microbiota: a hidden player in polycystic ovary syndrome. *Journal of Translational Medicine*, *23*(1), 443. https://doi.org/10.1186/s12967-025-06315-7

Shen, Y., Zhao, H., Wang, X., Wu, S., Wang, Y., Wang, C., Zhang, Y., & Zhao, H. (2024). Unraveling the web of defense: the crucial role of polysaccharides in immunity. *Frontiers in Immunology*, *15*. https://doi.org/10.3389/fimmu.2024.1406213

Silva, F. C. O., Araújo, M. I. F. de, Silva, S. P., Coelho, E., Santos, A. T. dos, González, A., Salvador, A. F. F., Cahú, T. B., Vieira, A. T., Souza, M. P. de, Coimbra, M. A., Teixeira, J. A., Nobre, C., Soares, P. A. G., & Correia, M. T. dos S. (2025). Structural characterization and in vitro gut microbiota fermentation of a polysaccharide extracted from Cenostigma nordestinum gum. *Carbohydrate Polymers*, *363*, 123738. https://doi.org/10.1016/j.carbpol.2025.123738

So, D., Whelan, K., Rossi, M., Morrison, M., Holtmann, G., Kelly, J. T., Shanahan, E. R., Staudacher, H. M., & Campbell, K. L. (2018). Dietary fiber intervention on gut microbiota composition in healthy adults: a systematic review and meta-analysis. *The American Journal of Clinical Nutrition*, *107*(6), 965–983. https://doi.org/10.1093/ajcn/nqy041

Song, Q., Cheng, S. W., Li, D., Cheng, H., Lai, Y. S., Han, Q., Wu, H. Y., Shaw, P. C., & Zuo, Z. (2022). Gut microbiota mediated hypoglycemic effect of Astragalus membranaceus polysaccharides in db/db mice. *Frontiers in Pharmacology*, *13*. https://doi.org/10.3389/fphar.2022.1043527

Strain, C. R., Collins, K. C., Naughton, V., McSorley, E. M., Stanton, C., Smyth, T. J., Soler-Vila, A., Rea, M. C., Ross, P. R., Cherry, P., & Allsopp, P. J. (2020). Effects of a polysaccharide-rich extract derived from Irish-sourced Laminaria digitata on the composition and metabolic activity of the human gut microbiota using an in vitro colonic model. *European Journal of Nutrition*, *59*(1), 309–325. https://doi.org/10.1007/s00394-019-01909-6

Sun, D., Qu, J., Huang, Y., Lu, J., & Yin, L. (2021). Analysis of microbial community diversity of muscadine grape skins. *Food Research International*, *145*, 110417. https://doi.org/10.1016/j.foodres.2021.110417

Sun, Y., Hu, J., Zhang, S., He, H., Nie, Q., Zhang, Y., Chen, C., Geng, F., & Nie, S. (2021). Prebiotic characteristics of arabinogalactans during in vitro fermentation through multi-omics analysis. *Food and Chemical Toxicology*, *156*, 112522. https://doi.org/10.1016/j.fct.2021.112522

Tan, J., McKenzie, C., Potamitis, M., Thorburn, A. N., Mackay, C. R., & Macia, L. (2014). *The Role of Short-Chain Fatty Acids in Health and Disease* (pp. 91–119). https://doi.org/10.1016/B978-0-12-800100-4.00003-9

Throat, S., & Bhattacharya, S. (2025). The Role of RS Type 2 (High-Amylose Maize Starch) in the Inhibition of Colon Cancer: A Comprehensive Review of Short-Chain Fatty Acid (SCFA) Production and Anticancer Mechanisms. *Molecular Nutrition & Food Research*. https://doi.org/10.1002/mnfr.70107

Tian, S., Paudel, D., Hao, F., Neupane, R., Castro, R., Patterson, A. D., Tiwari, A. K., Prabhu, K. S., & Singh, V. (2023). Refined fiber inulin promotes inflammation-associated colon tumorigenesis by modulating microbial succinate production. *Cancer Reports*, *6*(11). https://doi.org/10.1002/cnr2.1863

Ullah, H., Alioui, Y., Liu, X., Ali, S., Tang, B., Lu, H., Ruan, Y., & Hu, X. (2025). Deglet Noor date derived polysaccharides lower blood glucose levels and modulate the gut microbiota in a streptozotocin-induced type-1 diabetic mouse model. *Food & Function*. https://doi.org/10.1039/D5FO00128E

Villares, A. (2013). Polysaccharides from the edible mushroom Calocybe gambosa: structure and chain conformation of a (1→4),(1→6)-linked glucan. *Carbohydrate Research*, *375*, 153–157. https://doi.org/10.1016/j.carres.2013.04.017

Vuralli, D., Ceren Akgor, M., Dagidir, H. G., Onat, P., Yalinay, M., Sezerman, U., & Bolay, H. (2024). Microbiota alterations are related to migraine food triggers and inflammatory markers in chronic migraine patients with medication overuse headache. *The Journal of Headache and Pain*, *25*(1), 192. https://doi.org/10.1186/s10194-024-01891-3

Wang, B. H., Cao, J. J., Zhang, B., & Chen, H. Q. (2019). Structural characterization, physicochemical properties and α-glucosidase inhibitory activity of polysaccharide from the fruits of wax apple. *Carbohydrate Polymers*, *211*. https://doi.org/10.1016/j.carbpol.2019.02.006

Wang, L., Li, L., Gao, J., Huang, J., Yang, Y., Xu, Y., Liu, S., & Yu, W. (2021). Characterization, antioxidant and immunomodulatory effects of selenized polysaccharides from dandelion roots. *Carbohydrate Polymers*, *260*. https://doi.org/10.1016/j.carbpol.2021.117796

Wang, L., Liu, H. M., Xie, A. J., Wang, X. De, Zhu, C. Y., & Qin, G. Y. (2018). Chinese quince (Chaenomeles sinensis) seed gum: Structural characterization. *Food Hydrocolloids*, *75*. https://doi.org/10.1016/j.foodhyd.2017.08.001

Wang, L., Zhang, B., Xiao, J., Huang, Q., Li, C., & Fu, X. (2018). Physicochemical, functional, and biological properties of water-soluble polysaccharides from Rosa roxburghii Tratt fruit. *Food Chemistry*, *249*, 127–135. https://doi.org/10.1016/j.foodchem.2018.01.011

Wang, M., Wichienchot, S., He, X., Fu, X., Huang, Q., & Zhang, B. (2019). In vitro colonic fermentation of dietary fibers: Fermentation rate, short-chain fatty acid production and changes in microbiota. *Trends in Food Science & Technology*, *88*, 1–9. https://doi.org/10.1016/j.tifs.2019.03.005

Wang, N., Jia, G., Wang, X., Liu, Y., Li, Z., Bao, H., Guo, Q., Wang, C., & Xiao, D. (2021). Fractionation, structural characteristics and immunomodulatory activity of polysaccharide fractions from asparagus (Asparagus officinalis L.) skin. *Carbohydrate Polymers*, *256*, 117514. https://doi.org/10.1016/j.carbpol.2020.117514

Wu, J., Yu, C., Shen, S., Ren, Y., Cheng, H., Xiao, H., Liu, D., Chen, S., Ye, X., & Chen, J. (2023). RGI-Type Pectic

Polysaccharides Modulate Gut Microbiota in a Molecular Weight-Dependent Manner In Vitro. *Journal of Agricultural and Food Chemistry*, *71*(4), 2160–2172. https://doi.org/10.1021/acs.jafc.2c07675

Wu, Z.-W., Liu, X.-C., Quan, C.-X., Tao, X.-Y., Yi-Luo, Zhao, X.-F., Peng, X.-R., & Qiu, M.-H. (2025). Novel galactose-rich polysaccharide from Ganoderma lucidum: structural characterization and immunomodulatory activities. *Carbohydrate Polymers*, *362*, 123695. https://doi.org/10.1016/j.carbpol.2025.123695

Xia, X., Lu, J., Chen, X., Zhou, L., Huang, Y., Ding, S., & Li, G. (2024). Impact of whole grain highland hull-less barley on the denaturing gradient gel electrophoresis profiles of gut microbial communities in rats fed high-fat diets. *Microbiology Spectrum*, *12*(6). https://doi.org/10.1128/spectrum.04089-23

Xiong, Y., Cheng, Z., Zhang, Y., Liu, T., Wan, Z., Xia, C., Zhou, B., Shan, C., Song, D., & Miao, F. (2025). Ellagic acid alleviates DSS–induced ulcerative colitis by inhibiting ROS/NLRP3 pathway activation and modulating gut microbiota in mice. *European Journal of Nutrition*, *64*(1), 64. https://doi.org/10.1007/s00394-024-03577-7

Xu, Y., Chen, J., Shi, S., Gao, W., Wu, J., Gong, H., Zhao, Y., Chen, W., Wang, H., & Wang, S. (2023). Structure characterization of pectin from the pollen of Typha angustifolia L. and the inhibition activity of lipid accumulation in oleic acid induced L02 cells. *Carbohydrate Polymers*, *303*, 120452. https://doi.org/10.1016/j.carbpol.2022.120452

Yang, C.-J., Chang, H.-C., Sung, P.-C., Ge, M.-C., Tang, H.-Y., Cheng, M.-L., Cheng, H.-T., Chou, H.-H., Lin, C.-Y., Lin, W.-R., Lee, Y.-S., & Hsieh, S.-Y. (2024). Oral fecal transplantation enriches Lachnospiraceae and butyrate to mitigate acute liver injury. *Cell Reports*, *43*(1), 113591. https://doi.org/10.1016/j.celrep.2023.113591

Yang, X., Wei, S., Lu, X., Qiao, X., Simal-Gandara, J., Capanoglu, E., Woźniak, Ł., Zou, L., Cao, H., Xiao, J., Tang, X., & Li, N. (2021). A neutral polysaccharide with a triple helix structure from ginger: Characterization and immunomodulatory activity. *Food Chemistry*, *350*. https://doi.org/10.1016/j.foodchem.2021.129261

Yang, Z., Su, Q., Yang, J., Li, Z., Lan, S., Jia, X., Ouyang, P., & Tang, H. (2025). Effects of Dietary Tea Polyphenols on the Growth, Antioxidant Status, Immune Function, and Intestinal

Microbiota of Largemouth Bass (Micropterus salmoides). *Animals*, *15*(2), 222. https://doi.org/10.3390/ani15020222

Yokota, H., Tanaka, Y., & Ohno, H. (2025). Coculture of *Bifidobacterium bifidum* G9-1 With Butyrate-Producing Bacteria Promotes Butyrate Production. *Microbiology and Immunology*. https://doi.org/10.1111/1348-0421.13224

Yue, F., Zhang, J., Xu, J., Niu, T., Lü, X., & Liu, M. (2022). Effects of monosaccharide composition on quantitative analysis of total sugar content by phenol-sulfuric acid method. *Frontiers in Nutrition*, *9*. https://doi.org/10.3389/fnut.2022.963318

Zeng, F., Chen, W., He, P., Zhan, Q., Wang, Q., Wu, H., & Zhang, M. (2020). Structural characterization of polysaccharides with potential antioxidant and immunomodulatory activities from Chinese water chestnut peels. *Carbohydrate Polymers*, *246*, 116551. https://doi.org/10.1016/j.carbpol.2020.116551

Zhai, Y., Zhang, Z., Li, Y., Zhao, C., Peng, Z., Liu, Y., & Yang, P. (2025). Preparation, structural characterization, and bioactivities of polysaccharides from Rhodiola: A review. *International Journal of Biological Macromolecules*, *307*, 141873. https://doi.org/10.1016/j.ijbiomac.2025.141873

Zhang, H., Li, C., Ding, J., Lai, P. F. H., Xia, Y., & Ai, L. (2020). Structural features and emulsifying stability of a highly branched arabinogalactan from immature peach (Prunus persica) exudates. *Food Hydrocolloids*, *104*. https://doi.org/10.1016/j.foodhyd.2020.105721

Zhang, H., Li, C., Lai, P. F. H., Chen, J., Xie, F., Xia, Y., & Ai, L. (2021). Fractionation, chemical characterization and immunostimulatory activity of β-glucan and galactoglucan from Russula vinosa Lindblad. *Carbohydrate Polymers*, *256*. https://doi.org/10.1016/j.carbpol.2020.117559

Zhang, Y., Ma, Y., Fan, Y., Gao, Y., He, Y., Wang, Y., Nan, B., Liu, J., Li, X., & Wang, Y. (2024). Lactobacillus plantarum LP104 improved intestinal and brain inflammation by modulating TLR4 pathway and gut flora in alcohol liver injury mice. *Food Bioscience*, *62*, 105424. https://doi.org/10.1016/j.fbio.2024.105424

Zhao, T., Liu, S., Shuai, Y., Zhang, X., Chen, M., Pei, S., Duan, Y., Wang, S., Lu, Y., Wang, Z., Gong, G., & Huang, L. (2025). Influence of in vitro pectin fermentation on the human fecal microbiome and O-glycosylation of HT29-MTX cells. *International Journal of Biological Macromolecules*, *284*, 137710. https://doi.org/10.1016/j.ijbiomac.2024.137710

Zhao, Y., Wen, J., Yang, Y., Jia, L., Ma, Q., Jia, W., & Qi, W. (2025). *In vitro* fermentation characteristics of polysaccharide from *Scrophularia ningpoensis* and its effects on type 2 diabetes mellitus gut microbiota. *PeerJ*, *13*, e19374. https://doi.org/10.7717/peerj.19374

Zhi, N., Chang, X., Zha, L., Zhang, K., Wang, J., & Gui, S. (2025). Platycodonis radix polysaccharides suppress progression of high-fat-induced obesity through modulation of intestinal microbiota and metabolites. *Phytomedicine*, *142*, 156653. https://doi.org/10.1016/j.phymed.2025.156653

Zhou, J., Wei, H., Zhou, A., Xiao, X., Xie, X., Tang, B., Lin, H., Tang, L., Meng, R., Yuan, X., Zhang, J., Huang, C., Huang, B., Liao, X., Zhong, T., He, S., Gu, S., & Yang, S. (2024). The gut microbiota participates in the effect of linaclotide in patients with irritable bowel syndrome with constipation (IBS-C): a multicenter, prospective, pre-post study. *Journal of Translational Medicine*, *22*(1), 98. https://doi.org/10.1186/s12967-024-04898-1

Zhou, S., Huang, G., & Chen, G. (2021). Extraction, structural analysis, derivatization and antioxidant activity of polysaccharide from Chinese yam. *Food Chemistry*, *361*. https://doi.org/10.1016/j.foodchem.2021.130089

Zhu, L., Gong, H., Gan, X., Bu, Y., Liu, Y., Zhang, T., Chen, J., Xu, Y., Shi, S., Li, T., Li, B., Wang, S., & Wang, H. (2025). “Processing-structure-activity” relationships of polysaccharides in Chinese Materia Medica: A comprehensive review. *Carbohydrate Polymers*, *358*, 123503. https://doi.org/10.1016/j.carbpol.2025.123503

Zhu, Z., Luo, Y., Lin, L., Gao, T., Yang, Q., Fan, Y., Wang, S., Fu, C., & Liao, W. (2024). Modulating Effects of Turmeric Polysaccharides on Immune Response and Gut Microbiota in Cyclophosphamide-Treated Mice. *Journal of Agricultural and Food Chemistry*, *72*(7), 3469–3482. https://doi.org/10.1021/acs.jafc.3c05590

Fig. 1 Extraction, isolation and purification of the almond polysaccharide AS-3. Extraction and isolation of AS-3 (A); Chromatogram purified by DEAE-52 cellulose column (B)； Chromatogram of purification by Sephadex G-100 dextran gel column (C). The UV–vis spectra of AS-3 (D); Absolute molecular weight of AS-3 (E); Molecular configuration of AS-3 (F).

Fig. 2 Diagram of the monosaccharide composition of AS-3, (1: fucose, 2: rhamnose, 3: arabinose, 4: galactose, 5: glucose, 6: xylose, 7: mannose, 8: fructose, 9: ribose, 10: galacturonic acid, 11: guluronic acid, 12: glucuronic acid, 13: mannuronic acid) (A); FT-IR diagram of AS-3 (B); AS-3 SEM image with a magnification of 500Í (C); with a magnification of 5000Í (D) Analysis of the triple-stranded helical structure of AS-3 (E)

Fig. 3 NMR spectra of AS-3. ^{1}H-NMR (A), ^{13}C-NMR (B), COSY (C), NOESY (D), HSQC (E) and HMBC (F) Structure of AS-3 (G).

Fig. 4 Changes in pH value of fermentation broth (A); Changes in SCFAs production (B); Changes in alpha diversity, Sparse curve (C); abundance rank curve (D); variation in CHAO1 index, Shannon index, Simpson index, Goods coverage index (E); Beta diversity analysis, PCoA (F); Venn diagram (G). BLK: no carbon source group, AS: AS-3 treated group, INL: inulin treated group.

Fig. 5 Effect of AS-3 fermentation for 24h and 48h on microbial species, phylum level analysis (A), family level analysis (B), genus level analysis (C); Differential bacteria analysis, species composition heatmap (D), LEfSe analysis (E), LDA (F); Spearman correlation analysis, correlation analysis of AS-3 fermentation 24h

(G) and 48h (H) SCFAs and genus level flora. BLK: no carbon source group, AS: AS-3 treated group, INL: inulin treated group.

Declaration of interests

☒ The authors declare that they have no known competing financial interests or personal relationships that could have appeared to influence the work reported in this paper.

☐ The authors declare the following financial interests/personal relationships which may be considered as potential competing interests:

Graphical abstract

Highlights

1. AS-3 from almond shows a prebiotic effect on healthy individuals' intestinal flora.
2. Structurally, AS-3 is a 50.956 kDa polysaccharide with a triple helical structure and specific linkages.
3. AS-3 boosts microbial diversity better than inulin, increases SCFAs like acetic/butyric acid.
4. It promotes beneficial bacteria, inhibits harmful ones, and reduces the Firmicutes/Bacteroidetes ratio.
5. AS-3 has potential for functional food development and intestinal microecology intervention.

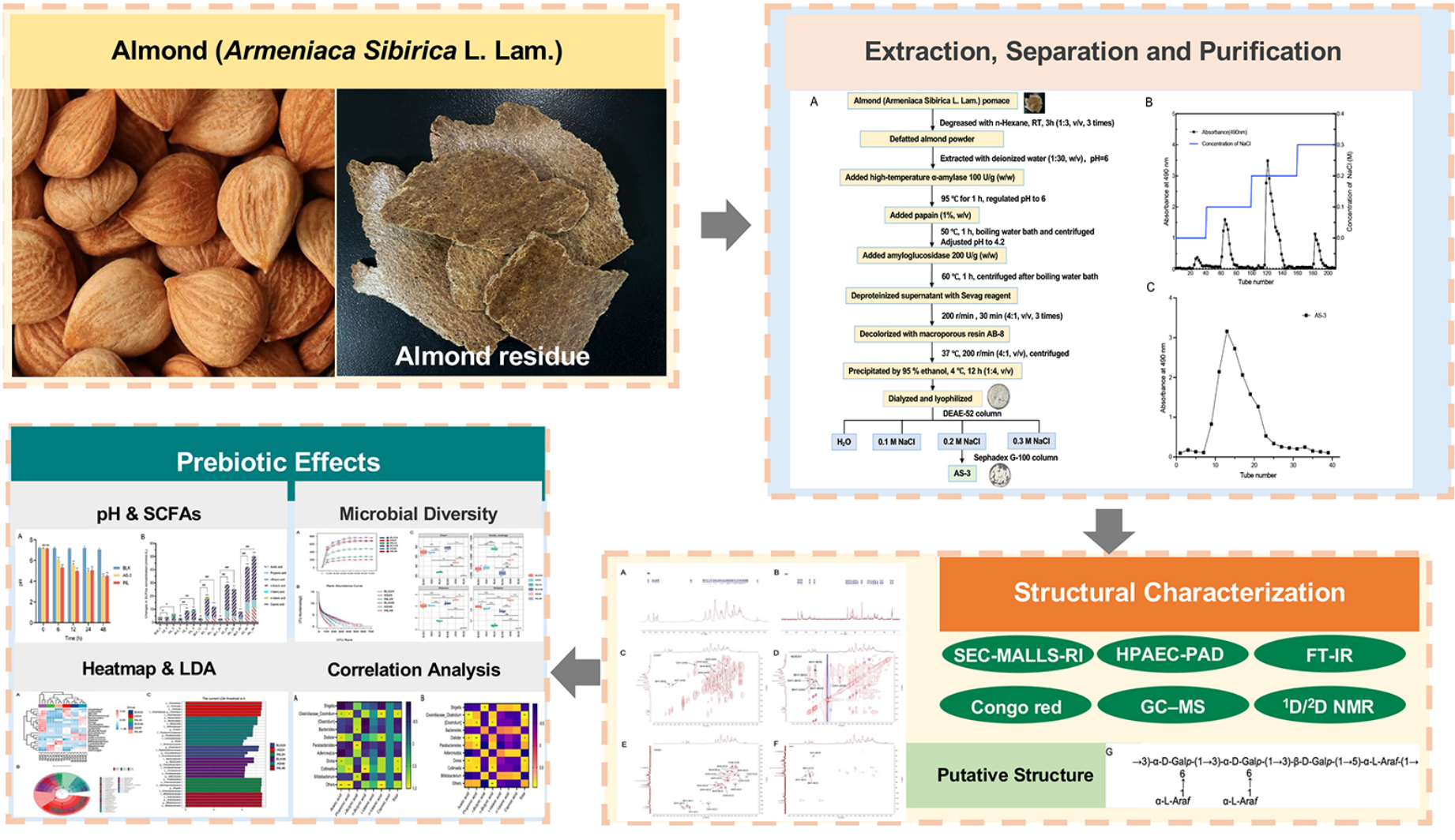

Graphics Abstract

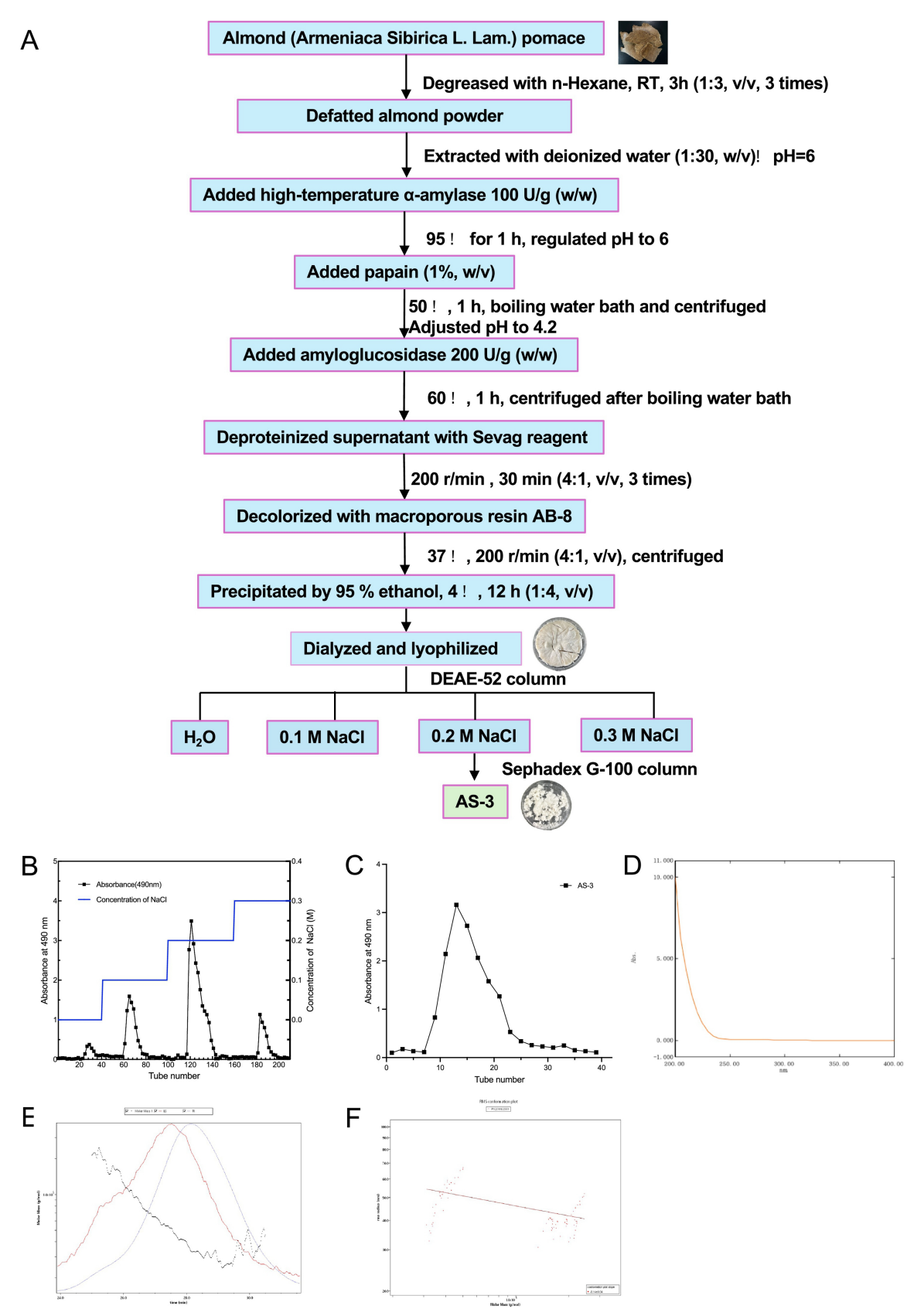
A
Almond (Armeniaca Sibirica L. Lam.) pomace
Degreased with n-Hexane, RT, 3h (1:3, v/v, 3 times)
Defatted almond powder
Extracted with deionized water (1:30, w/v)！ pH=6
Added high-temperature α-amylase 100 U/g (w/w)
95！ for 1 h, regulated pH to 6
Added papain (1%, w/v)
50！, 1 h, boiling water bath and centrifuged
Adjusted pH to 4.2
Added amyloglucosidase 200 U/g (w/w)
60！, 1 h, centrifuged after boiling water bath
Deproteinized supernatant with Sevag reagent
200 r/min , 30 min (4:1, v/v, 3 times)
Decolorized with macroporous resin AB-8
37！, 200 r/min (4:1, v/v), centrifuged
Precipitated by 95 % ethanol, 4！, 12 h (1:4, v/v)
Dialyzed and lyophilized
DEAE-52 column
H2O
0.1 M NaCl
0.2 M NaCl
0.3 M NaCl
Sephadex G-100 column
AS-3
B
Absorbance(490nm)
Concentration of NaCl
Absorbance at 490 nm
Concentration of NaCl (M)
Tube number
C
AS-3
Absorbance at 490 nm
Tube number
D
E
F

Figure 1

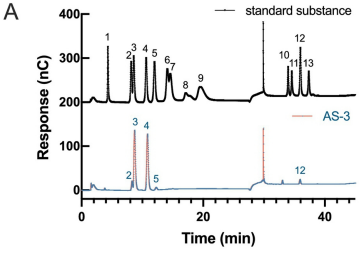
A
standard substance
AS-3
Response (nC)
Time (min)
1
2
3
4
5
6
7
8
9
10
11
12
13

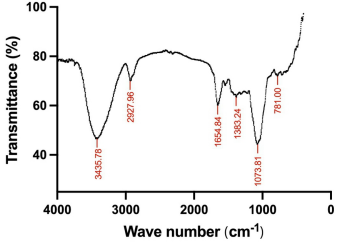
B
Transmittance (%)
Wave number (cm-1)
3435.78
2927.96
1654.84
1383.24
1073.81
781.00

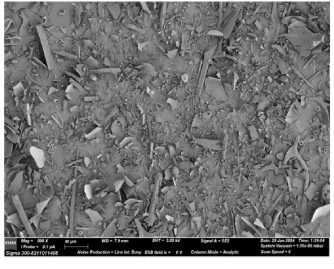
C


D

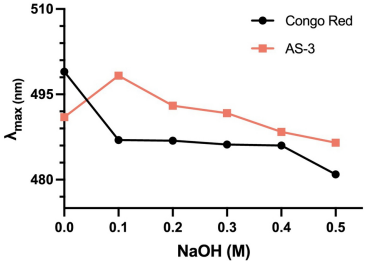
E
Congo Red
AS-3
λmax (nm)
NaOH (M)

Figure 2

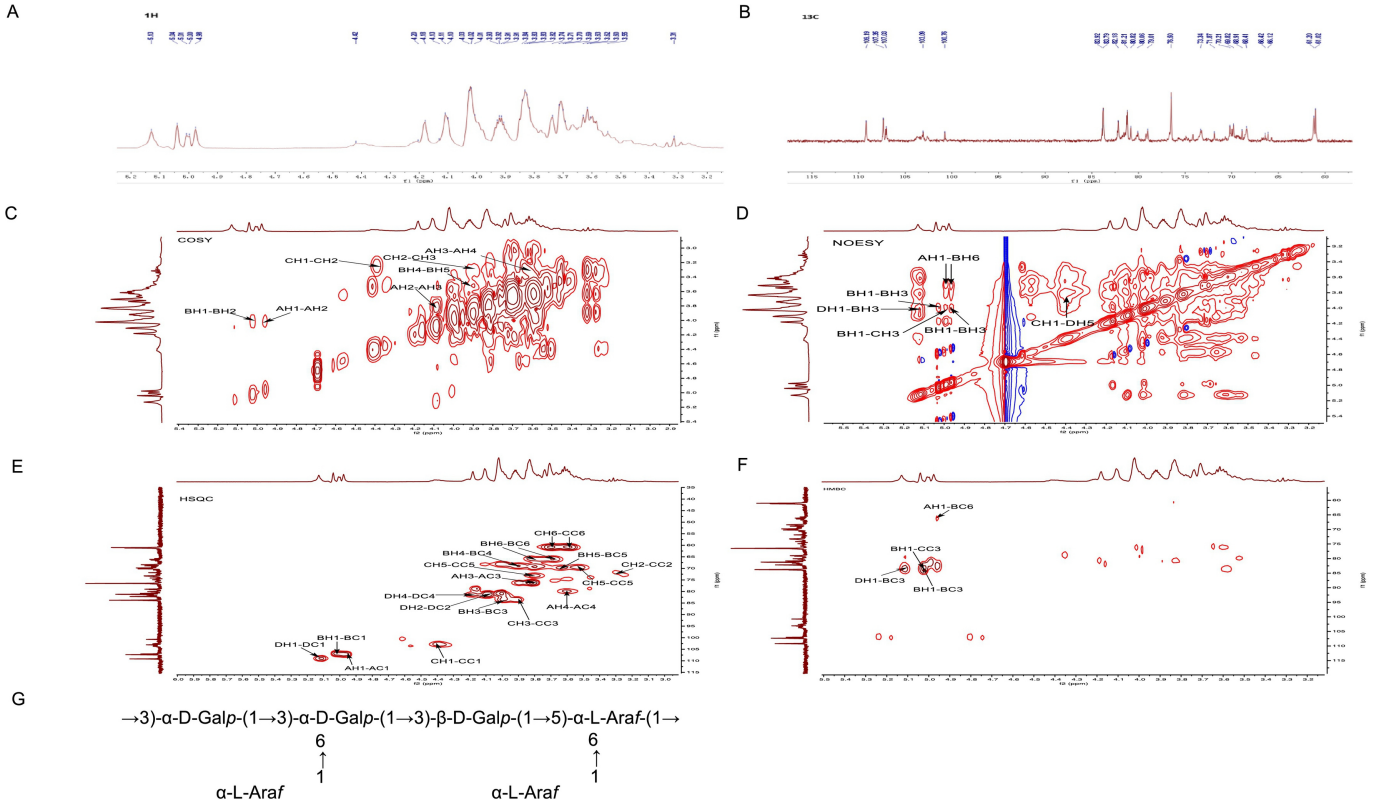
A
1H
B
13C
C
COSY
CH1-CH2
CH2-CH3
AH3-AH4
BH4-BH5
AH2-AH3
BH1-BH2
AH1-AH2
D
NOESY
AH1-BH6
BH1-BH3
DH1-BH3
BH1-CH3
BH1-BH3
CH1-DH5
E
HSQC
CH6-CC6
BH6-BC6
BH4-BC4
BH5-BC5
CH5-CC5
CH2-CC2
AH3-AC3
CH5-CC5
DH4-DC4
DH2-DC2
BH3-BC3
AH4-AC4
CH3-CC3
BH1-BC1
DH1-DC1
AH1-AC1
CH1-CC1
F
HMBC
AH1-BC6
BH1-CC3
DH1-BC3
BH1-BC3
G
→3)-α-D-Gal*p*-(1→3)-α-D-Gal*p*-(1→3)-β-D-Gal*p*-(1→5)-α-L-Ara*f*-(1→
6
1
α-L-Ara*f*
6
1
α-L-Ara*f*

Figure 3

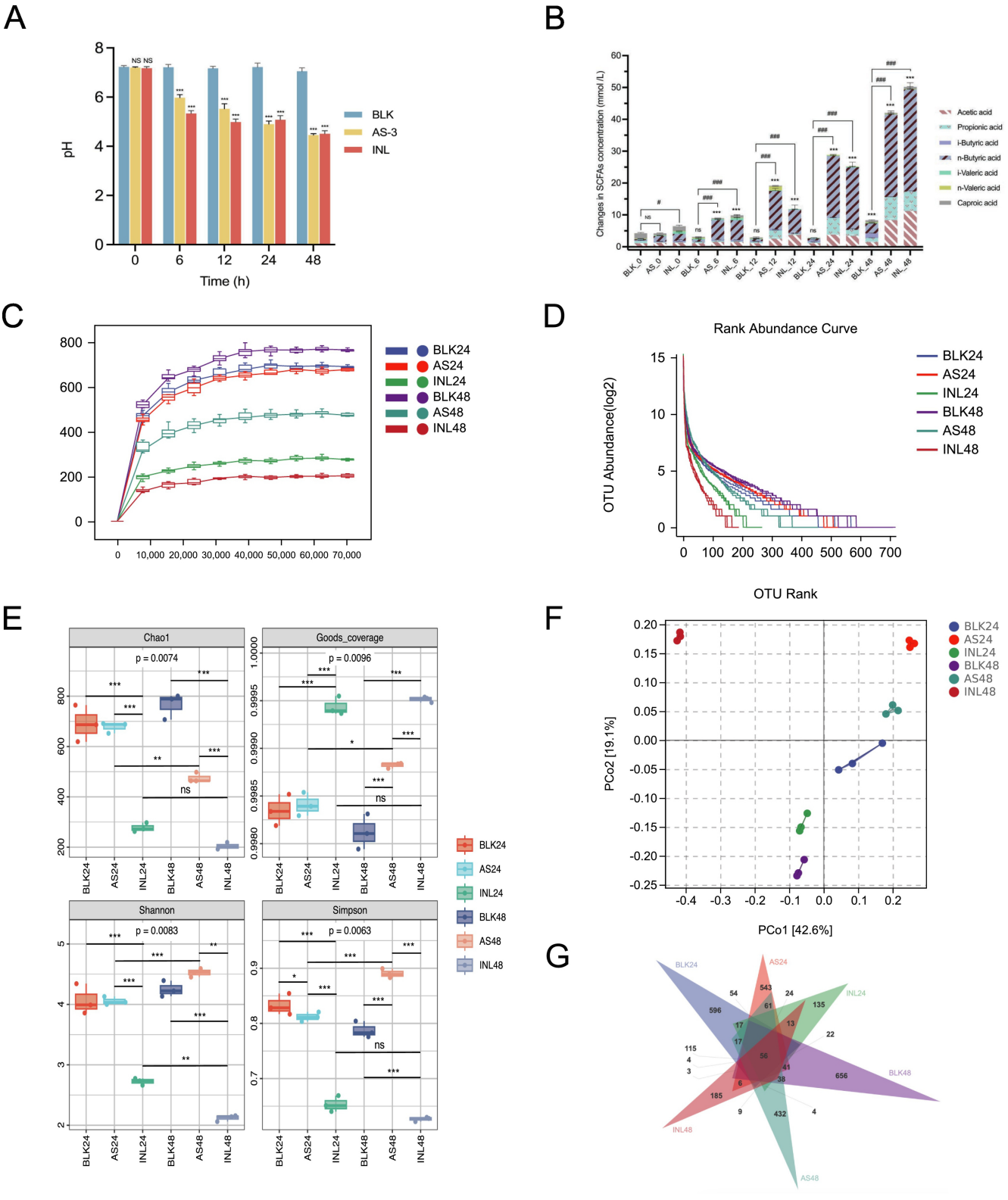
A
pH
Time (h)
BLK
AS-3
INL
B
Changes in SCFAs concentration (mmol /L)
Acetic acid
Propionic acid
i-Butyric acid
n-Butyric acid
i-Valeric acid
n-Valeric acid
Caproic acid
C
BLK24
AS24
INL24
BLK48
AS48
INL48
D
Rank Abundance Curve
OTU Abundance(log2)
OTU Rank
E
Chao1
p = 0.0074
Goods_coverage
p = 0.0096
Shannon
p = 0.0083
Simpson
p = 0.0063
F
PCo2 [19.1%]
PCo1 [42.6%]
G

Figure 4

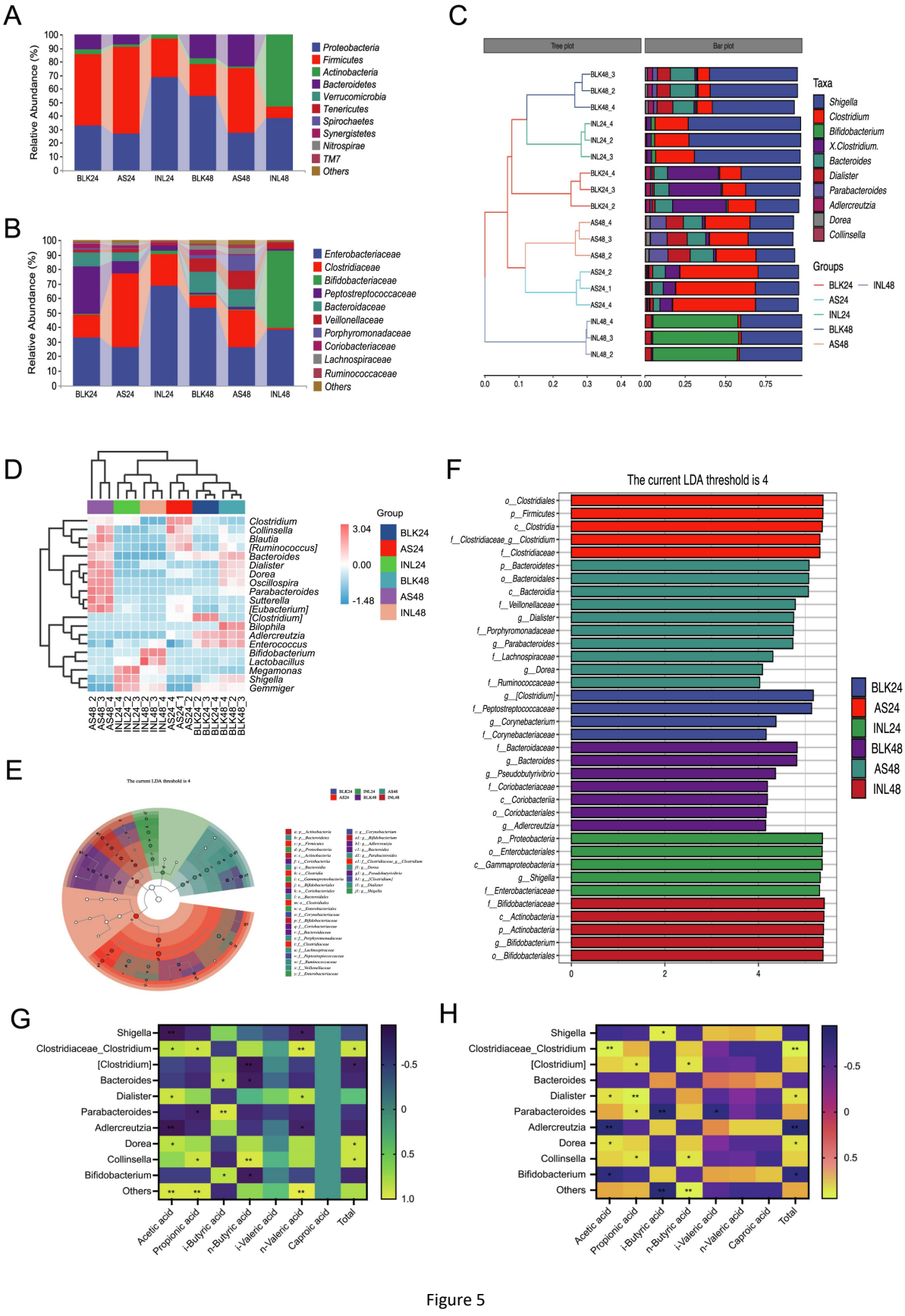
A
Relative Abundance (%)
BLK24
AS24
INL24
BLK48
AS48
INL48
Proteobacteria
Firmicutes
Actinobacteria
Bacteroidetes
Verrucomicrobia
Tenericutes
Spirochaetes
Synergistetes
Nitrospirae
TM7
Others
B
Relative Abundance (%)
Enterobacteriaceae
Clostridiaceae
Bifidobacteriaceae
Peptostreptococcaceae
Bacteroidaceae
Veillonellaceae
Porphyromonadaceae
Coriobacteriaceae
Lachnospiraceae
Ruminococcaceae
Others
C
Tree plot
Bar plot
Taxa
Shigella
Clostridium
Bifidobacterium
X.Clostridium.
Bacteroides
Dialister
Parabacteroides
Adlercreutzia
Dorea
Collinsella
Groups
BLK24
INL48
AS24
INL24
BLK48
AS48
D
Group
3.04
0.00
-1.48
BLK24
AS24
INL24
BLK48
AS48
INL48
Clostridium
Collinsella
Blautia
[Ruminococcus]
Bacteroides
Dialister
Dorea
Oscillospira
Parabacteroides
Sutterella
[Eubacterium]
[Clostridium]
Bilophila
Adlercreutzia
Enterococcus
Bifidobacterium
Lactobacillus
Megamonas
Shigella
Gemmiger
E
The current LDA threshold is 4
F
The current LDA threshold is 4
o__Clostridiales
p__Firmicutes
c__Clostridia
f__Clostridiaceae.g__Clostridium
f__Clostridiaceae
p__Bacteroidetes
o__Bacteroidales
c__Bacteroidia
f__Veillonellaceae
g__Dialister
f__Porphyromonadaceae
g__Parabacteroides
f__Lachnospiraceae
g__Dorea
f__Ruminococcaceae
g__[Clostridium]
f__Peptostreptococcaceae
g__Corynebacterium
f__Corynebacteriaceae
f__Bacteroidaceae
g__Bacteroides
g__Pseudobutyrivibrio
f__Coriobacteriaceae
c__Coriobacteriia
o__Coriobacteriales
g__Adlercreutzia
p__Proteobacteria
o__Enterobacteriales
c__Gammaproteobacteria
g__Shigella
f__Enterobacteriaceae
f__Bifidobacteriaceae
c__Actinobacteria
p__Actinobacteria
g__Bifidobacterium
o__Bifidobacteriales
BLK24
AS24
INL24
BLK48
AS48
INL48
G
Shigella
Clostridiaceae_Clostridium
[Clostridium]
Bacteroides
Dialister
Parabacteroides
Adlercreutzia
Dorea
Collinsella
Bifidobacterium
Others
-0.5
0
0.5
1.0
Acetic acid
Propionic acid
i-Butyric acid
n-Butyric acid
i-Valeric acid
n-Valeric acid
Caproic acid
Total
H
Shigella
Clostridiaceae_Clostridium
[Clostridium]
Bacteroides
Dialister
Parabacteroides
Adlercreutzia
Dorea
Collinsella
Bifidobacterium
Others
-0.5
0
0.5
Acetic acid
Propionic acid
i-Butyric acid
n-Butyric acid
i-Valeric acid
n-Valeric acid
Caproic acid
Total

Figure 5